Norwegian University
of Life Sciences

Master's Thesis 2024 60 ECTS
Faculty of Veterinary Medicine

Development of transgenic lines to study pituitary cell development and plasticity in medaka (*Oryzias latipes*)

Leon Nathaniel Stellander
Biotechnology

DEVELOPMENT OF TRANSGENIC LINES TO STUDY PITUITARY CELL DEVELOPMENT AND PLASTICITY IN MEDAKA (*ORYZIAS LATIPES*)

BY

Leon Nathaniel Stellander

SUPERVISOR

Romain Fontaine

CO-SUPERVISOR

Arturas Kavaliauskis

MCs THESIS - BIOTECHNOLOGY

SUBMITTED TO THE FACULTY OF VETERINARY MEDICINE

NORWEGIAN UNIVERSITY OF LIFE SCIENCES

MAY 2024

Keywords: Transgenic, Gene editing, Fluorescent proteins, NTR, Plasticity, Regeneration, Tissue Culture, Oryzias latipes, Pituitary, Hormones, Fsh, Tsh

Acknowledgements

First of all, I would like to thank everyone who have helped me on the pathway of finishing this project. Additionally, I want to express my appreciation for the amazing people which have made me feel welcome during this period. With a lot of different experiments, followed new and unforeseen problems. These would not have been solved without the fantastic people I have been surrounded with these last two years.

I want to express my gratitude to all the Drs. in our group who has helped me troubleshoot and progress in my master's thesis. Without Rasoul Nourizadeh-Lillabadi, Simona Kavaliauskiene and Muhammad Rahmad Royan I would not have been able to inject all my medaka eggs or be able to screen them. Our PhD candidates Ida Helene Kallevik and Evgenia Dunaevskaya have motivated me and included me in their exciting projects (Even though I'm good at blood sampling from humans, I can now confidently say the same about salmon, thanks to Ida). I wish you both well on your PhDs! To engineers Anders Høkedal, Anthony Peltier and Sudip Mahat, thank you for all the help and lighthearted moments this last year.

Lastly, it is worth mentioning my amazing supervisors Dr. Romain Fontaine and Dr. Arturas Kavaliauskis. When times have been extremely busy, you have never hesitated to prioritize helping and including me. Your supervision has broken me down to build me even stronger (and hopefully smarter). Thanks for all the wisdom, patience, laughter, and encouragement. I hope the transgenic lines we developed come to good use, and that a lot of exciting knowledge will be discovered.

The last year has made me grow into a more independent person, thanks to all the experiences and people I have encountered. Thanks to my friends, family and partner for always believing and supporting me.

Sincerely,

Leon

Abstract

The reproductive system is an important process highly regulated by hormones produced by the pituitary gland, including the thyroid-stimulating hormone (Tsh) and the follicle-stimulating hormone (Fsh). The pituitary is a highly plastic organ and adapts hormone production according to their demand. The mechanisms involved in this plasticity are poorly known, same as their regulation. To further study the development and plasticity of these endocrine cell populations, this project developed two new transgenic lines in the model fish Japanese medaka (*Oryzias latipes*).

First, a transgenic line named tg(*tshbb*:tdTomato) was produced, in which the gene encoding the fluorescent protein tdTomato was under the control of the *tshbb* promoter. This line allowed us to visualize the cells expressing the *tshbb* gene of which the function and location remain mostly unknown to this day. A fluorescent cell population was observed between the eyes in developing transgenic medaka larvae. This could hopefully indicate that Tshbb expression has successfully been visualized for the first time in this species, whereas further studies are needed to characterize this endocrine cell population.

Second, a transgenic line named tg(*fshb*:NTR-CFP/*fshb*:DsRed2) carried the gene encoding the bacteria-derived protein nitroreductase and the fluorescence proteins CFP and DsRed2 under the control of the *fshb* promoter. Nitroreductase expression is known to induce cell-specific apoptosis when treated with ronidazole. With these properties, the transgenic line could be useful for investigating regeneration of removed tissue. Dissected brain- and pituitary tissue was kept in specific culture conditions which were shown to minimize tissue degradation. In these conditions, high-concentration treatments of ronidazole demonstrated to ablate Fsh cells. Regeneration of these cells was unfortunately not observed in this project, so more studies are needed to characterize their role in pituitary plasticity.

Further development of the transgenic lines developed in this study will allow deeper investigation of these two endocrine cell populations of the pituitary gland. The unknown function of Tshbb may finally be discovered, and the regeneration of Fsh cells may be explored deeper in the medaka.

Sammendrag

Det reproduktive systemet er en viktig prosess som er sterkt regulert av hormoner fra hypofysen, inkludert thyreoideastimulerende hormon (Tsh) og follikkelstimulerende hormon (Fsh). Hypofysen er et svært plastisk organ og tilpasser hormonproduksjon etter behov. De involverte mekanismene og reguleringene av denne plastisiteten er hittil lite utforsket. For å ytterligere studere utviklingen og plastisiteten til disse endokrine cellepopulasjonene, utviklet dette prosjektet to nye transgene linjer av modellfisken japansk medaka (*Oryzias latipes*).

Først ble en transgen linje kalt tg(*tshbb*:tdTomato) produsert, der genet som koder for fluorescensproteinet tdTomato var under kontroll av *tshbb*-promotoren. Denne linjen gjorde det mulig å visualisere cellene som uttrykker *tshbb*-genet, som til dags dato har ukjent funksjon og lokasjon. En fluorescerende cellepopulasjon ble observert mellom øynene hos transgene medaka-yngel i utvikling. Dette kan forhåpentligvis indikere at Tshbb-uttrykket har blitt visualisert for første gang i denne arten, men ytterligere studier er nødvendig for å karakterisere denne endokrine cellepopulasjonen.

For det andre bar en transgen linje kalt tg(*fshb*:NTR-CFP/*fshb*:DsRed2) genet som koder for det bakteriederiverte proteinet nitroreduktase og fluorescensproteinene CFP og DsRed2 under kontroll av *fshb*-promotoren. Nitroreduktase-uttrykk er kjent for å indusere cellespesifikk apoptose ved ronidazol-stimulering. Med disse egenskapene kan den transgene linjen være nyttig for å undersøke regenerering av fjernet vev. Dissekert hjerne- og hypofysevev ble oppbevart i spesifikke kulturforhold som viste seg å minimere vevsdegradering. Under disse forholdene viste høykonsentrasjonsbehandlinger av ronidazol seg å fjerne Fsh-celler. Regenerering av disse cellene ble dessverre ikke observert i dette prosjektet, så flere studier er nødvendig for å karakterisere deres rolle i hypofysens plastisitet.

Videreutvikling av de transgene linjene som ble dannet i denne studien, vil tillate dypere undersøkelser av disse to endokrine cellepopulasjonene i hypofysen. Den ukjente funksjonen til Tshbb kan endelig bli oppdaget, og regenereringen av Fsh-celler kan utforskes nærmere hos medaka.

Table of Contents

Abbreviations

Abbreviation	Explanation
BP	Brain-pituitary
CFP	Cyan fluorescent protein
DAPI	4′,6-diamidino-2-phenylindole
DMSO	Dimethyl sulfoxide
dPBS	Dulbecco’s phosphate-buffered saline
Dpf	Day(s) post fertilization
DSB	Double-strand break
FSH	Follicle-stimulating hormone
GFP	Green fluorescent protein
GH	Growth hormone
GMO	Genetically modified organisms
GnRH	Gonadotropin-releasing hormone
HDR	Homology-directed repair
INDELs	Insertions and deletions
LB	Lysogeny broth
LH	Luteinizing hormone
LP	Long light period
Mpf	Minute(s) post fertilization
α-MSH	Melanocyte-stimulating hormone
MTZ	Metronidazole
NTR	Nitroreductase
nfsB	NAD(P)H-dependent Nitroreductase (NTR gene)
PBST	Phosphate-buffered saline-Tween
Pc	Compensation pressure
PCR	Polymerase chain reaction
PFA	Paraformaldehyde
Pi	Injection pressure
POMC	Pro-opiomelanocortin
PRL	Prolactin
RFP	Red fluorescent protein

RZ	Ronidazole
SL	Somatolactine
Sox2	Sex determining region Y-box 2
SP	Short light period
T3	Triiodothyronine
T4	Thyroxine
TAE	Tris-acetate-EDTA
TRH	Thyroid-releasing hormone
TSH	Thyroid-stimulating hormone
WT	Wildtype

Specific Nomenclature

Molecule	Mammalian	Fish	Full name
Protein	FSH	Fsh	Follicle-stimulating hormone
Gene	*(FSHB)*	*fshb*	*Follicle-stimulating hormone subunit beta*
Protein	(GnRH)	Gnrh	Gonadotropin-releasing hormone
Protein	LH	Lh	Luteinizing hormone
Gene	*(LHB)*	*lhb*	*Luteinizing hormone subunit beta*
Protein	(SOX2)	Sox2	Sex determining region Y-box 2
Protein	TSH	Tsh	Thyroid-stimulating hormone
		Tshba	Thyroid-stimulating hormone subunit beta a
		Tshbb	Thyroid-stimulating hormone subunit beta b
Gene	*TSHB*	*tshba*	*Thyroid-stimulating hormone subunit beta [a]*
		tshbb	*Thyroid-stimulating hormone subunit beta b*

Terms

Term	Explanation
Ablation	Cell- or tissue removal/destruction
Atlantic salmon	*Salmo salar*
Brine shrimp	*Artemia salina*
Differentiation	Recruitment of progenitor cells
E. coli	*Escherichia coli*
Ex vivo	“Outside of the living”
F0	Founder generation
F1	Generation 1
F2	Generation 2
Gonadotrope	Cell type
Gonadotropin	Hormone
In vivo	“Inside of the living”
Intercrossing	Reproduction between fish belonging to the same generation
Medaka	*Oryzias latipes*
Out-crossing	Reproduction with wildtype fish
Photoperiod	Daylight length
Sex steroids	Reproductive hormones produced by the gonads (testosterone; progesterone; and estradiol)
Tg(*fshb*:DsRed2)	Transgenic *fshb* line
Tg(*fshb*:NTR-CFP/*fshb*:DsRed2)	Transgenic *fshb* line
Tg(*tshbb*:tdTomato)	Transgenic *tshbb* line
Transdifferentiation	Phenotypic change
T	Hemizygous genotype
Tt	Heterozygous genotype
TT	Homozygous positive genotype
tt	Homozygous negative genotype
Zebrafish	*Danio rerio*

1. Introduction

1.1 The pituitary gland

The hypophysis, (also named the pituitary gland) is a lobular structure located ventrally on the hypothalamus of the vertebrate brain (1). It consists of the anterior and posterior lobes, known as the adenohypophysis and neurohypophysis, respectively. While the neurohypophysis mainly consists of neurosecretory fibers, nerve terminals, and glia-like supportive cells, the adenohypophysis contains several different endocrine cells secreting peptide hormones (2). These secretory cells include the somatotropes (producing growth hormone, GH), gonadotropes (producing the gonadotropins luteinizing hormone, LH; and follicle-stimulating hormone, FSH), lactotropes (producing prolactin, PRL), thyrotropes (producing thyroid-stimulating hormone, TSH), melanotropes (producing melanocyte-stimulating hormone, α-MSH) and corticotropes (producing pro-opiomelanocortin, POMC). Teleost fish possess an additional cell type, the somatolactotropes (producing somatolactine, SL) (3). The locations of these endocrine cell populations vary between different classes of vertebrates (Figure 1). Whereas mammalian endocrine cells have a mosaic distribution within the pituitary (except for melanotropes), teleost cells are divided into distinct populations (1,4). Another difference between fish and other vertebrates is that fish gonadotropins are mostly produced in separate Lh and Fsh cells (5).

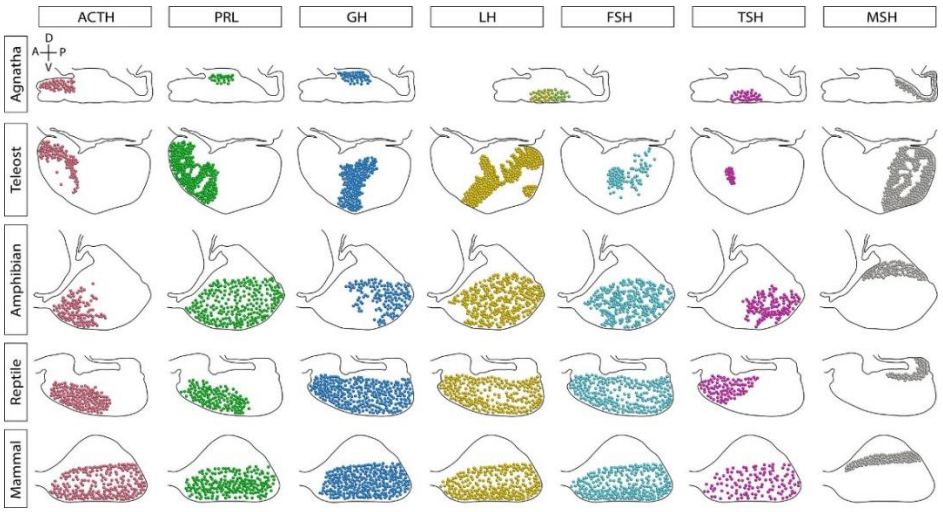

Figure 1: The endocrine cell distribution in the vertebrate pituitary gland. While mammals show mosaic distributions in most pituitary endocrine cells, other classes like the teleosts show more clustered populations of cell types (1).

The pituitary hormones are part of the brain-pituitary (BP) axis, which forms a multitude of neuroendocrine pathways that regulate essential physiological functions, such as homeostasis and reproduction (see Figure 2). In this neuroendocrine system, the hypothalamus part of the brain regulates the hormone production and release of pituitary endocrine cells in response to internal- and external signals. For instance, thyroid-releasing hormone (TRH) and gonadotropin-releasing hormone (GnRH) stimulate hormone production and secretion from the thyrotrope and gonadotrope cells, respectively. This results in the secretion of TSH by thyrotropes and LH and FSH by gonadotropes (6–8). These three glycoprotein hormones consist of an α-subunit which they share, and a β-subunit which is hormone-specific and provides the specific endocrine function (9).

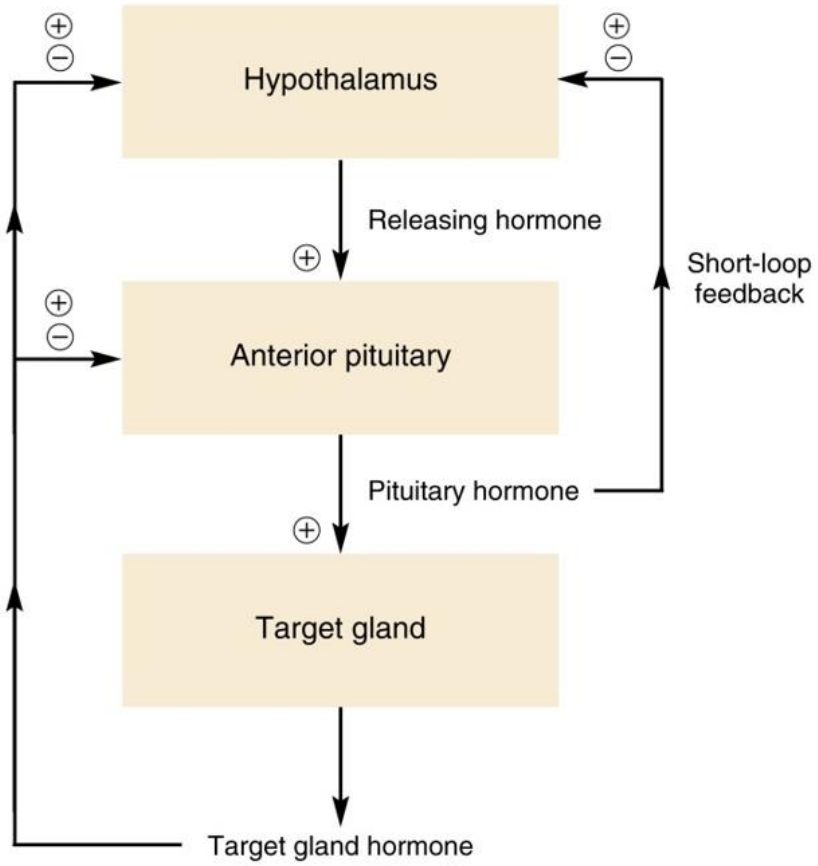

Figure 2: The BP axis consists of the hypothalamus in the brain, the pituitary (and the gonads). Top panel: The hypothalamus stimulates the anterior pituitary with, for instance, GnRH. Middle panel: GnRH stimulates the gonadotropes of the anterior pituitary to produce the gonadotropins. Excess of gonadotropins can induce negative and positive feedback loops to regulate the hypothalamus. Bottom panel: Gonadotropins also stimulate the target gonads to produce sex steroids which are important for reproduction. An excess of sex steroids can create negative and positive feedback to the hypothalamus and anterior pituitary to up- or downregulate their stimulation. Adapted from Hiller-Sturmhöfel et al. (10).

TSH targets the thyroid gland and stimulates the production of the thyroid hormones triiodothyronine (T3) and thyroxine (T4), which control the metabolism, heart rate, body temperature, and homeostasis (6). Teleosts have gone through a whole-genome duplication, which resulted in two Tsh genes encoding the β-subunit, *tshba* and *tshbb*. Both the homology and the functions of *tshba* is similar to the mammalian *TSHB* gene, which include control of development, growth, and metabolism. Additionally, teleost *tshba* is involved in osmoregulation and gonadotropin regulation (11,12). There are very few studies about *tshbb* and its function. A recent study by Fleming et al. (13) suggested that the *tshbb* gene expression peaks during smoltification in the Atlantic salmon (*Salmo salar*), being regulated by daylight length, also called photoperiod (14,15). Knowledge about the function of *tshbb* in non-smoltifying species is sparse, but in the medaka (*Oryzias latipes*) it has been suggested to be involved as a paracrine factor in photoperiod regulation (14). Extensive investigation is still needed for this *tshbb* gene.

The gonadotropes, LH and FSH are important reproductive hormones that stimulate the production of sex steroids (testosterone; progesterone; and estrogens) in the gonads. LH stimulates testosterone release by the Leydig cells in the testes in males. In females, however, LH stimulates androgen release in the ovaries, which is converted to estradiol, responsible for ovulation. The estradiol conversion would not be possible without FSH, which also stimulates the production of enzymes critical for ovulation (16,17). FSH is critical for the gametogenesis and follicle development of female ovaries whereas in males, FSH is necessary for maintaining normal sperm count and function (18). The production of these hormones must be carefully regulated to obtain optimal function. For instance, the timing of the gonadotropin production is crucial for the onset of reproduction for seasonally reproducing species.

The regulation of gonadotropin hormones depends heavily upon a complex interplay between negative- and positive feedback loops and many contributing factors. The endocrine feedback loops are important regulators of hormone production. For instance, sex steroids produced by the gonads will up- or down-regulate hormone production in the pituitary and the brain. The ability of the pituitary to regulate these feedback loops are important for meeting the hormone demands of an organism throughout its life cycle (19).

1.1.1 Pituitary plasticity

The pituitary is a very plastic organ. The different hormone productions can be adjusted to meet the demand either by regulating cell activity (production and release) or by changing the cell numbers of different endocrine cell populations. The hormone production (mRNA and proteins) and hormone-releasing activity have been widely studies and shown to heavily depend on input from the brain (such as GnRH stimulation), the positive- and negative-feedback loops from circulating sex steroids (see Figure 2), and from cell-to-cell communication within the pituitary (20,21). On the other hand, change in cell number of hormone-producing cells has been poorly investigated. Several mechanisms co-exist, including recruitment of progenitor cells (differentiation), mitosis of mature endocrine cells, phenotypic change (transdifferentiation), and apoptosis as illustrated in Figure 3.

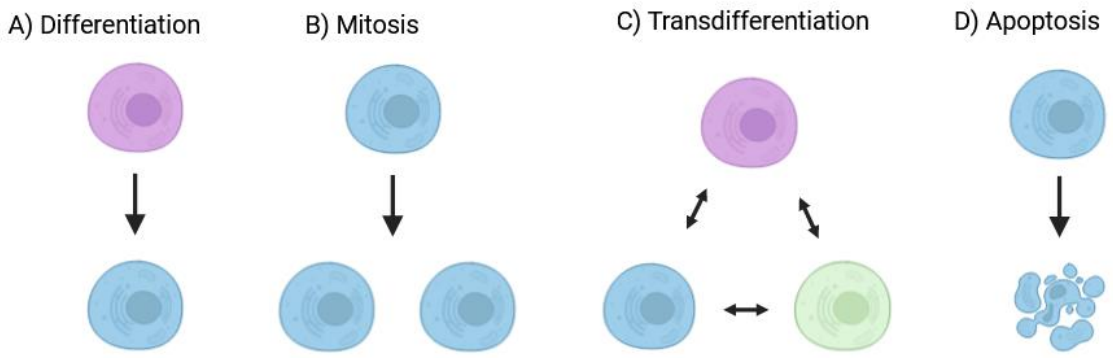

Figure 3: Simplified illustration of important mechanisms of regulating cell number in cell plasticity. A) Differentiation matures a cell from a progenitor (purple) cell into a mature and specialized cell (blue). B) Mitosis increases cell number by dividing a mature cell (blue) into two identical daughter cells. C) Transdifferentiation is the conversion from one specialized cell to another (green), either through dedifferentiation to a progenitor cell which again differentiates, or direct conversion. D) Apoptosis is the reduction of cells through programmed cell death (Made in Biorender).

These mechanisms affecting the change in cell number are important for the development of a fertilized egg, and throughout the development of a species. When an egg is fertilized it develops into a totipotent stem cell, meaning this cell has the potential to become any cell of an organism (22). Differentiation, mitosis, transdifferentiation and apoptosis are heavily involved in the further development of cells and tissue. The maturation of stem cells and progenitor cells is essential to increase populations of desired cell types of an organism (23). The progenitor- and stem cells can be recruited to the demanding tissue to differentiate into specialized cells.

Mitosis occurs when a mature somatic mother cell divides into two phenotypically identical daughter cells and is a natural mechanism of the cell cycle. Mitosis rates can be increased or decreased according to the demand of the pituitary cells. For instance, some recent studies showed that mature endocrine cells have the capacity to go through mitosis in the model fish medaka (24).

For a long time, it was believed that when cells matured, they would permanently stay in their role until apoptosis. Mature cells can also in some cases dedifferentiate by re-entering the cell cycle and return to its state as a progenitor cell. Additionally, it has recently been discovered that cells can change phenotype to replace other cell types and their roles to meet physiological demands (25). This is called transdifferentiation, and usually involves an intermediate dedifferentiation step into a progenitor cell, which later differentiates into another cell within the same lineage or into a new lineage of cells (23). This was, for instance, demonstrated by Jopling et al. (26), where amputated zebrafish (*Danio rerio*) heart tissue regenerated through dedifferentiation of neighboring cardiomyocytes, which later differentiated into new heart tissue. The damaged tissue was hence regenerated and restored.

Apoptosis is a mechanism that decreases the number of cells and is part of the natural cell cycle. It is also referred to as programmed cell death and is an important cellular process to remove sick or damaged cells to later replace them with new and healthy tissue by the previously mentioned mechanisms (27). These processes which allow for tissue plasticity are important to understand in order to investigate the pituitary and its remarkable adaptability.

1.2 The Japanese medaka as a model organism

The Japanese medaka (Figure 4) is a small freshwater teleost fish and thus part of the largest vertebrate class with approximately 30,000 species (28). Medaka is native to China, Japan, and Korea with a natural habitat in rice fields (29).

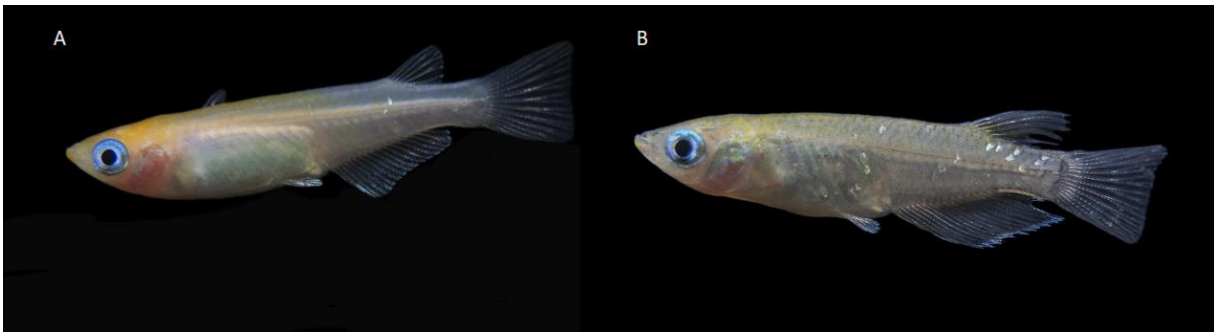

Figure 4: Female (A) and male (B) adult medaka. Adapted from Aquatic Arts© (30).

As a small oviparous fish, the medaka produces transparent eggs (Figure 5), has a short generation time of 2 months, and has an adult size of approximately 2.5 cm which makes it easy to raise in laboratory conditions (31). It is worth noting that like other fish, the medaka has the remarkable ability to regrow tissue upon amputation. It has been well demonstrated that if the tip of the caudal fin is amputated, the tissue will regenerate after a given time (32). Therefore, this also makes the medaka a good model to study tissue plasticity. In addition, because of the numerous tools available to study its biology and development, medaka is widely used in research (33). For instance, its genome is entirely sequenced, which makes it a practical model species for genome editing (34). In addition, contrary to the well-known model fish, zebrafish, medaka has a less complex and shorter genome, making gene studies easier (35,36). Interestingly, medaka has a closer phylogenetic relationship to the Atlantic salmon than the zebrafish, making it an important model species for the seafood industry (37).

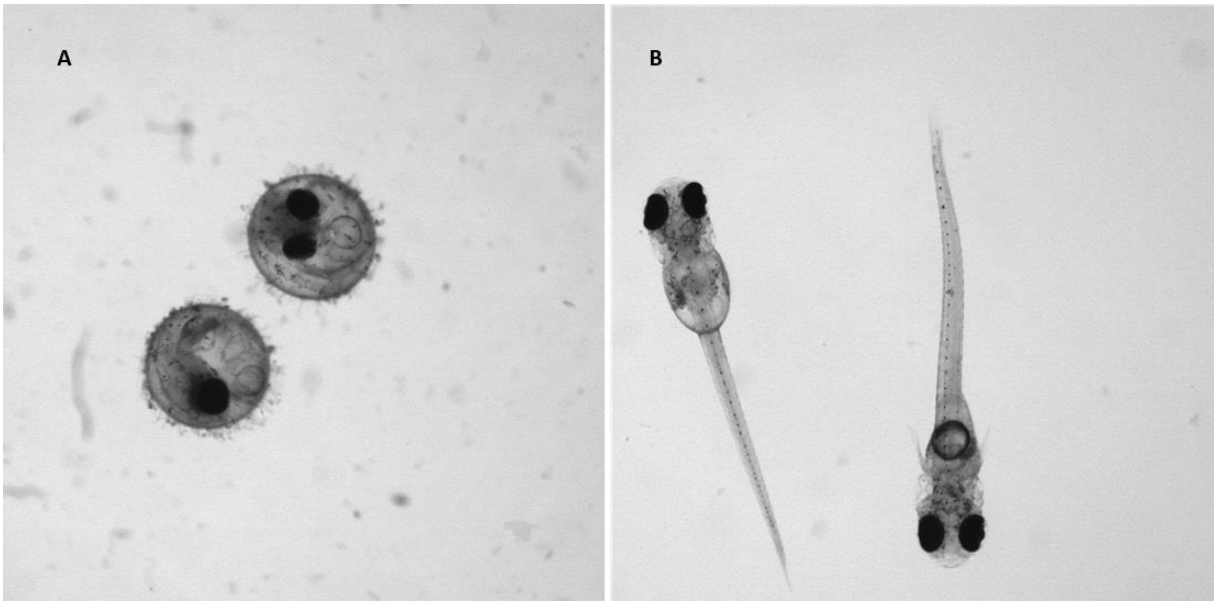

Figure 5: Medaka fry are still transparent in the egg stage (A) at 6 days post fertilization and the larvae stage (B) at 9 days post fertilization (Magnification 2x).

1.2.1 Proliferation and pituitary plasticity in medaka

Recent studies in medaka have especially focused on the pituitary cell plasticity and its ability to adapt to stimuli. This has been advanced by mapping out the location of essential endocrine- and non-endocrine cells in a 3D atlas of the juvenile, female, and male medaka pituitary (5). The creation of this map revealed that the expression of the *fshb, lhb* and *tshba* genes significantly increase from juvenile to adult stages in female medaka. Additionally, proliferation of gonadotropes and Tshba-cells was shown. This suggests that the proliferation of these gonadotrope and thyrotrope cells, and their increase in hormone expression, occur at puberty. The gonadotropes and thyrotropes are important cells that regulate reproduction. Recent studies demonstrated that extended periods of photoperiod stimulated internal pathways, such as Tsh stimulation of gonadotropin expression and gonadotrope proliferation, implying that Tsh is involved in the plasticity of gonadotropes (14).

There are several plasticity mechanisms investigated in the medaka, including differentiation of progenitor cells, mitosis, and transdifferentiation. In two studies by Fontaine et al., it was shown that the hyperplasia of gonadotrope cells may be caused by Lh cell mitosis. Additionally, it was suggested that the gonadotropes had the capability of transdifferentiation. Indeed, bi-hormonal Fsh cells co-expressing Lh were observed, suggesting that Fsh cells can transdifferentiate to Lh cells or develop bi-hormonal properties. Finally, sex determining

region Y-box 2 (Sox2) progenitor cells were suspected to differentiate into Fsh cells in males, suggesting that the progenitor cells participated in Fsh cell proliferation through their recruitment (24,38).

The regulation of these pituitary plasticity mechanisms has been further investigated and includes stimulation by sex steroids. As previously mentioned, gonadotropes produce gonadotropins, which in turn stimulate the gonads to produce sex steroids. The sex steroids impact the production of gonadotropins through feedback-loops. By performing a gonadectomy, this sex steroid production would cease, thus allowing for investigation of the impact on the endocrine feedback loops and how hormone demand is obtained. Royan et al. (39) investigated how sex steroids affected the plasticity of Fsh cells after gonadectomy in medaka. The study demonstrated that the absence of sex steroid production is correlated with an upregulation of Fsh transcription. Additionally, Tsh cells also started to co-express Fsh in females, illustrating the impact of sex steroid stimulation of pituitary cell plasticity. Furthermore, the absence of sex steroids reduced the population and activity Sox2 progenitor cells in males, suggesting that the progenitor cells participated in Fsh cell proliferation through their recruitment. It is worth noting that the tissues of the medaka bear a higher proportion of Sox2 stem cells compared to mammals, suggesting a pool of progenitor cells fit for proliferation of, for instance, gonadotropes (40).

The regulation of the gonadotropes in the medaka is not only regulated by internal signals such as sex steroid stimulation but also by external signals, like photoperiod. Another study by Royan et al. (41) investigated how daylight length affected reproduction, gonadotrope populations, and gonadotropin secretion. In that study, medaka were raised under short- (SP) and long periods (LP) of daylight. SP females showed a significant decrease in spawning rates, whereas LP conditions improved gonadal development, mitosis-driven gonadotrope proliferation, and gonadotropin transcription levels. This demonstrated how LP greatly stimulates gonadotrope activity and proliferation.

Furthermore, the origin of increased transcription activity and gonadotrope hyperplasia was investigated. As previously mentioned, teleost fish including medaka, possess two paralog genes for the mammalian *TSHB*, called *tshba* and *tshbb* (12). While *tshba* has shown similar function as the mammalian gene, the function of *tshbb* is unknown. The study revealed that in female medaka raised in LP conditions, *tshba* expression was upregulated, while *tshbb* was

downregulated to undetectable levels. When treating whole pituitary tissue from these fish with mammalian TSH, proliferation markers were downregulated. In contrast, females raised in SP conditions had increased transcription levels of *tshbb*. Treatment of whole pituitary tissue from SP females with mammalian TSH resulted in both increased mitotic cells and mitotic gonadotropes. These findings suggest that the medaka Tsh genes are regulated by photoperiod. Additionally, as mammalian TSH and teleost Tshba share similar functions, it was suggested that *tshba* regulates gonadotrope mitosis and thus their activity.

1.2.2 The undiscovered role of tshbb

As described earlier, Royan et al. (41) highlighted how daylight length affected the *tshba* and *tshbb* expression levels. *Tshbb* levels were undetectable in long periods of daylight, while being increased in short daylight periods. A supplementary study by Royan et al. (14), hypothesized that melatonin levels are increased in short daylight conditions. Here, it was suggested that high melatonin levels indirectly suppressed *tshba* expression, but increased *tshbb* expression. As previously mentioned, Tshba stimulation of pituitaries from SP medaka increased gonadotrope mitosis. Since high melatonin levels from low light exposure indirectly downregulated *tshba* expression, it was suggested that SP had an inhibitory role on gonadotrope mitosis. While this illustrates the importance of *tshba* in reproduction, the function of *tshbb* in the regulation of gonadotrope plasticity remains unknown. In other species, like the Atlantic salmon, *tshbb* is downregulated in short daylight periods, in contrary to the medaka. However, *tshbb* has been suggested to stimulate gonadotropin production in response to long daylight exposure. Additionally, *tshbb* also plays a role in smoltification in Atlantic salmon (15). As the medaka is a non-smoltifying species, research regarding the endocrine role of *tshbb* in this species remains limited. Still, the pituitary gland of the medaka has demonstrated great adaptability of hormone production from other endocrine cells in response to both internal and external stimuli. By making transgenic lines of medaka, the role of *tshbb* in pituitary plasticity can finally be investigated in vivo.

1.3 Transgenic lines to investigate tissue development and plasticity

Transgenic animals have been used extensively as tools for studying for instance development and cell biology, the immune system in action, reproduction, and toxicology. The term “transgenic” was first introduced in 1981 by Gordon and Ruddle when attempting to inject DNA into the pronuclei of fertilized mouse oocytes. They discovered that the exogenous

gene, or the transgene, could be transmitted in a Mendelian distribution when passed on to mice progeny. This meant that editing the mice's genome also edited their offspring's genome (42).

A transgenic animal is thus an organism whose genome has been introduced to one or more exogenous DNA sequences from another species through genetic manipulation. Transgenic animals are considered genetically modified organisms (GMO) when introduced with transgenes, whereas older conventional ways include selective breeding of desirable traits or exposing the animal to mutating factors (43). In regard to optimizing time consumption and the specificity of gene editing, genetically modifying an organism is preferable.

By interbreeding transgenic animals, stable transgenic lines can be created. The transgene will be passed on to the next generation of progeny, ensuring new generations of transgenic animals. This has been done in various species like fruit flies (44), mice (45), sea urchins (46), frogs (47) and fish (48). Earlier transgenesis techniques of injecting only DNA yielded low success in creating transgenic lines (46). By inducing a double-strand break (DSB) in the target DNA (of the edited organism), the cell repair machinery would attempt to repair the cleavage in one of two ways. Random insertions and deletions (INDELs) or homology-directed repair (HDR) would undergo, depending on the absence or presence of a DNA template, respectively. These repair mechanisms are essential to understand when designing the vector that delivers the desired transgenes (49). Thermes et al. (50) demonstrated that supplying I-SceI meganuclease enzymes together with a plasmid containing a transgene, increased the probability of successful gene editing in medaka. During the last fifteen years, several transgenic medaka lines have been developed by using this approach. These were used to study the neuroendocrine system regulating reproduction, by labeling Gnrh, Lh, and Fsh cells with fluorescent reporter proteins (50–53).

Transgenic fluorescent lines that carry reporter proteins, such as cyan fluorescent proteins (CFP: like CFP) and red fluorescent proteins (RFP: like DsRed2 and tdTomato), have specifically been important for labeling, tracking, and quantifying cells expressing a gene of interest. Controlling these reporter proteins under the gene promoter of interest could allow for the traceability of this gene expression. Hildahl et al. (51) demonstrated that if the green fluorescent protein (GFP) is controlled by the Lh promoter, the expression of Lh can be visualized with GFP under the microscope. Here, the study showed that Lh expression during medaka larvae development could be traced with the GFP fluorescence. This Lh line has also

been used to determine the location and onset of gonadotrope cell development in the pituitary (24).

Recently, a new transgenesis approach has been used to study the plasticity of specific cell populations. Nitroreductase (NTR) is a protein (encoded by the *nfsB* gene) derived from *Escherichia coli* (*E. coli*) and has been used in experiments on targeted cell removal (ablation). When a cell expressing NTR is supplied with metronidazole (MTZ) or one of its derivatives, such as ronidazole (RZ), a cytotoxic environment is created, thus driving the cell into apoptosis (54). NTR has been used for targeted cell ablation in transgenic medaka for many cell types such as osteoblasts (55), neurons (56), and pancreatic β-cells (57).

Using transgenic lines as tools in biology research has been revolutionizing. These animals are important tools to model diseases, develop treatments, and study cell biology in a controlled laboratory environment (58). In vivo studies have allowed for more representative discoveries of gene expression in physiological processes. Additionally, transgenic lines can be continued through breeding programs which can ensure more transgenic subjects for future experiments.

1.4 Aim

The aim of this project was to develop transgenic lines of medaka to study the development and plasticity of two pituitary cell populations which have been shown to be interlinked, thyrotropes and gonadotropes, with the medaka as a model organism.

First, a transgenic medaka line with the fluorescent protein tdTomato under the control of the *tshbb* promoter, tg(*tshbb*:tdTomato), will be established. The line will help to investigate the function of Tshbb (NCBI gene ID: XP_011475459.1) and the development of this endocrine cell population. To this day the function, location, and development of Tshbb cells remain unknown. This will be achieved by gene editing medaka eggs through microinjection of the *tshbb*:tdTomato plasmid with I-SceI enzymes at one-cell stage embryos. Transgenic fish will participate in breeding programs of out-crossing with wildtype (WT) fish and intercrossing with transgenic fish.

Second, a transgenic medaka line co-expressing DsRed2, CFP, and NTR under the control of the *fshb* promoter tg(*fshb*:NTR-CFP/*fshb*:DsRed2) will also be established. This line will help investigate the plasticity of the Fsh gonadotrope population. As little research is done on the plasticity and regeneration of Fsh cells, there will be an attempt to remove these crucial cells with the NTR-system. The hypothesis is that the regenerative ability of the medaka will make the Fsh cells recover post-ablation. If they do recover, the pathways and mechanisms of this plasticity are yet to be identified.

In the future, these tools can help to better understand the pituitary and its hormones. In addition to better understanding the adaptability of the pituitary to the environment, these tools can unlock new knowledge about pituitary cell plasticity.

2. Methods

In this master's project, two transgenic lines of medaka were developed to study pituitary development and plasticity. To do this, medaka fish were genetically modified through microinjection of transgenes in combination with a specific restriction enzyme at the one-cell stage. Injected fish were raised until adulthood and screened with polymerase chain reaction (PCR) for positive individuals, before intercrossing them to establish the lines. Furthermore, one of the new lines were used in ex vivo experiments to demonstrate the practical properties of the transgene in the medaka pituitary.

2.1 Vector preparation

Two plasmids (Figure 6) were developed by the laboratory engineer, as described in the study by Hodne et al. (52). The first contained the gene encoding the fluorescent reporter protein tdTomato under the control of the endogenous *tshbb* promoter, to study the development of cells expressing *tshbb*. The second plasmid contained the gene encoding the NTR and the reporter protein CFP under the control of the *fshb* promoter to study the plasticity of cells expressing *fshb*. The plasmids also contained crucial sequences for successful transgenesis, including the homology flanking sequence, I-SceI cutting sites, and antibiotic resistance genes, enabling bacterial transformation for amplifying the plasmid. I-SceI is a rare-cutting meganuclease with a recognition site of 18-20 bp, making it specific when cutting genomic DNA. I-SceI additionally cleaves the transgene in the plasmid to create the homologous flanking site. This is essential for the repair machinery of the cell to undergo HDR and integrate the transgene into the genome.

2.1.1 Tshbb:Tomato plasmid

To create the transgenic line tg(*tshbb*:tdTomato), the dtTomato vector (*Takara Bio*) was digested by Ncol and Notl restriction enzymes (*New England BioLabs*) and cloned into the I-SceI-MCS-leader-Gfp-trailer plasmid (a gift from Karlsruhe Institute of Technology (KIT), Germany). This generated an I-SceI-MCS-leader-tdTomato-trailer vector. The medaka *tshbb* promoter was then amplified with overhang for the restriction enzymes Kpnl and Xhol before being purified with PCR. The promoter was then cloned into the pGEM-T Easy Vector

(*Promega*), before being digested with Kpnl and Xhol (*New England BioLabs*). This fragment was finally purified and cloned into cloned into the I-SceI-MCS-leader-tdTomato-trailer vector. This resulted in a plasmid expressing tdTomato under the control of the *tshbb* promoter, meaning that tdTomato fluorescence indicated *tshbb* expression (*tshbb:*tdTomato).

2.1.2 *Fshb*:NTR-CFP plasmid

To generate the tg(*fshb*:NTR-CFP/*fshb*:DsRed2) line, transgenic eggs from the established tg(*fshb*:DsRed2) line by Hodne et al. (52) would be edited by supplying a new plasmid. These transgenic fish expressed RFP controlled by the *fshb* promoter. The new plasmid vector was prepared similarly, as for the tg(*tshbb*:tdTomato) line. The NTR-CFP sequence (*Addgene,* (59)) and the medaka *fshb* promoter were amplified with overhang for the restriction enzymes Kpnl and Xhol before being purified with PCR. The sequence was then cloned into the pGEM-T Easy Vector, before being digested with Kpnl and Xhol. This fragment was purified and cloned into the I-SceI-MCS-leader-Gfp-trailer vector. This resulted in a plasmid expressing NTR and CFP under the control of the *fshb* promoter (*fshb:*NTR-CFP). Here, CFP fluorescence indicated NTR expression where *fshb* was expressed. When editing tg(*fshb*:DsRed2) eggs, the pre-existing *fshb*:DsRed2 transgene would additionally express RFP under the control of the *fshb* promoter. By containing two transgenes the edited tg(*fshb*:DsRed2) eggs would develop into tg(*fshb*:NTR-CFP/*fshb*:DsRed2) fish. Here, RFP would work as a control for the efficiency of *fshb:*NTR-CFP expression.

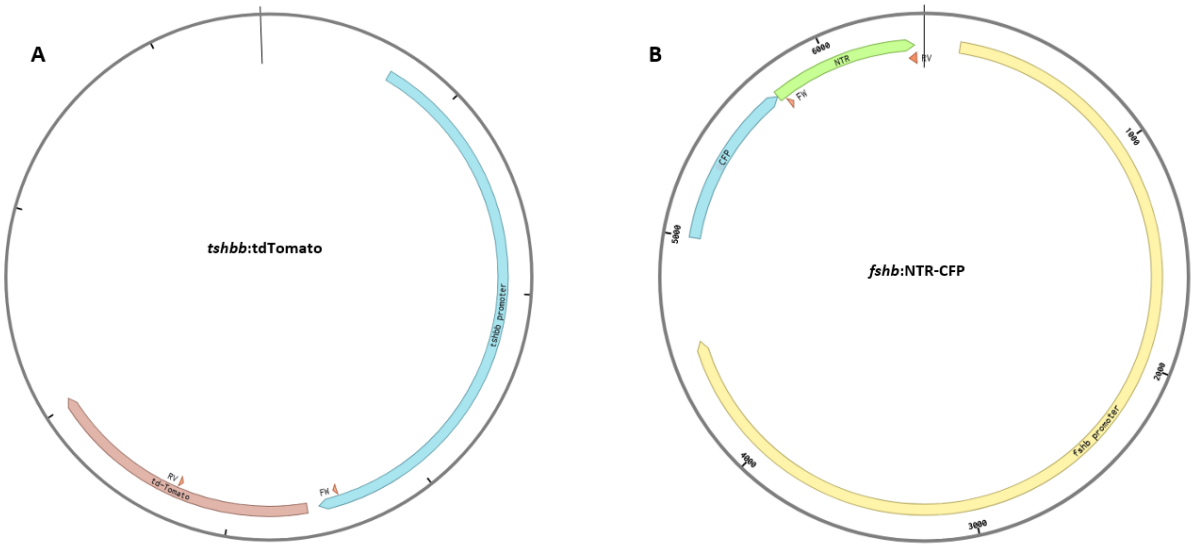

Figure 6: Simplified illustrations of the two developed vector plasmids. A) tshbb:tdTomato plasmid with the tshbb promoter (blue) and the tdTomato gene (red) with PCR primer locations (orange) B) The fshb:NTR-CFP plasmid with the fshb promoter (yellow), NTR gene (green), CFP gene (blue) and primer locations for PCR (orange) (Made in Benchling).

2.1.3 Bacterial transformation and plasmid amplification

The plasmids were amplified to ensure high quantities of injectant for future use. *E. coli* cells from the kit One Shot TOP10 Competent Cells (*Thermo Fischer*) were used to transform and amplify the plasmid according to the supplied protocol "Chemical Transformation Procedure". Here the *E. coli* cells received the vector plasmid through transformation and were spread on a prepared and labeled lysogeny broth (LB) agar plate containing Ampicillin for antibiotic resistance selection. The plate was inverted and incubated at 37 °C overnight. An approximately 2 cm stripe white bacterial colonies was collected with a sterile pipette tip and kept in collection tubes with 10 mL of LB medium before being left in the shaking incubator overnight at 225 rpm.

After incubation, the plasmid was extracted with the Plasmid DNA purification kit (*Macherey-Nagel*), with the supplied protocol "NucleoSpin Plasmid". Here the bacterial cells went through lysis, and the DNA was extracted following the manufacturer's instructions. The plasmid was collected in water and the DNA concentration was determined on an Epoch Microplate Spectrophotometer (*BioTek*), before being stored at -20 °C until use.

2.2 Rearing conditions in the model fish facility

The medaka of the WT d-rR strain and the tg(*fshb*:DsRed2) line (52), were used to generate transgenic medaka. The fish were kept in a long daylight cycle (14h daylight; 10h night) in recirculating water with an average system temperature of 27-28°C and a pH of 7.5. They were fed thrice daily, once with live brine shrimp larvae (*Artemia salina*), and twice with dry food. A maximum of twelve fish were housed in a 3.5-liter tank.

2.3 Egg production and collection

Several triadic groups of WT fish or tg(*fshb:*DsRed2) fish were formed. These consisted of two females and one male grouped in 3.5-liter tanks. The day before egg collection, old eggs were removed from the tank or the females (as they remain attached externally to the female body for some time after spawning in this species) and the females were separated from the male with a divider. In regulated laboratory lighting conditions, medaka spawn within one hour after the light is lit. By separating the male from the females, it is possible to control the spawning time. The next morning, the separating wall was removed soon after the light onset to initiate the mating ritual (60).

The mating ritual usually lasts 10-20 minutes, before the females release eggs and the male externally fertilizes them right away. For injection, it is important to collect the eggs as soon as possible after fertilization, as the first cell division begins 7-8 minutes post fertilization (mpf) and completes at approximately 60 mpf (61). It is indeed important to microinject one-cell stage eggs (Figure 7) to prevent a mosaic distribution of the transgene during embryonic development. To collect the eggs, the female was caught in a net, and a Pasteur pipette was used to safely remove the egg sack. The eggs were then dispensed into a petri dish containing system water. Since the eggs were stuck together in a fibrous network, the eggs were separated by twisting the egg sack fibers around two forceps. The Petri dish with the eggs was then placed on ice to slow down the egg development (62).

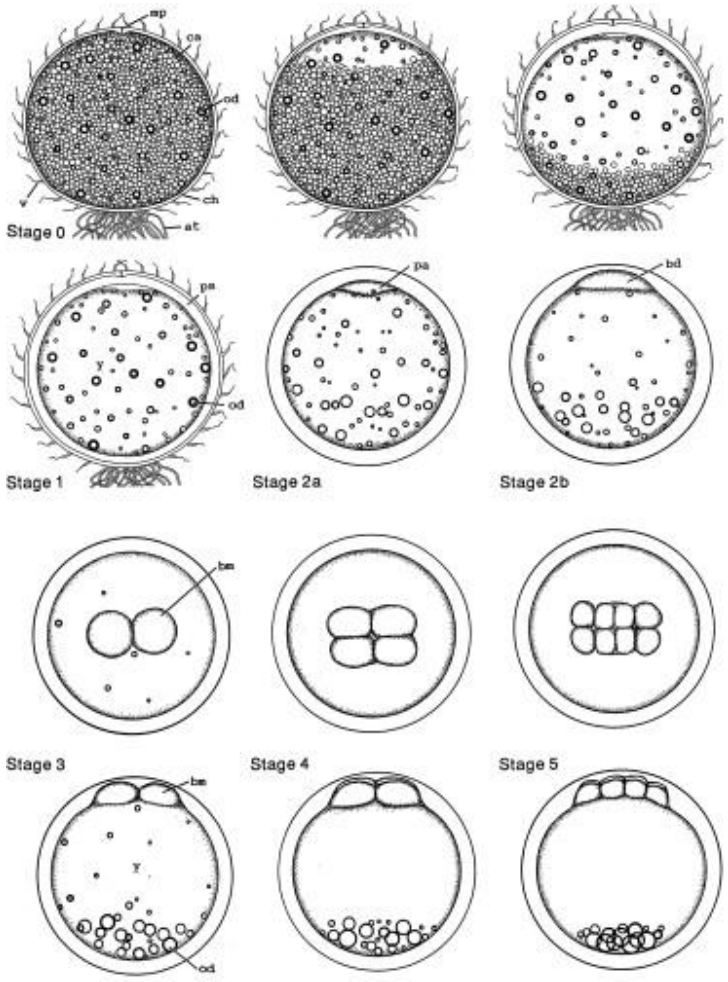

Figure 7: Stages of normal egg development in medaka. Egg fibers can be seen in the figures of stage 0 and 1 (at). The microinjection is done at the one-cell stage depicted in Stage 1-2b (bd) (61).

2.4 Microinjection

Prior to microinjection, an agar mold was made. The mold had grooves that fit the medaka eggs inside and was made by dissolving 3 g of agar in 100 mL of water, making 3% Electran Agarose DNA Grade agar (*VWR Chemicals*). The agar was solidified in the fridge for 10 minutes and the egg mold was filled with system water. Needles were made by stretching GD-1 Glass Capillaries with filament (*Narishige)*, having an outer diameter of 1.0 mm and inner diameter of 0.6 mm, on the P-1000 Micropipette Puller (*Stutter Instrument*). The needles were pulled with the following program: Heat 485; Pull 60; Vel 70; Time 250; Pressure 500. The tip was opened with forceps under the microscope to have a small enough opening to penetrate the eggs and still eject liquid.

The transgenic injectant was prepared by diluting the transgenic vector to 250 ng/µL of the *tshbb*:tdTomato plasmid, or 10 ng/µL for the *fshb:*NTR-CFP plasmid with 1 unit/µL I-SceI enzyme (*New England BioLabs*), rCutSmart Buffer (*New England BioLabs*) supplied with 0.1% phenol red to visualize the solution. The capillary needle was then loaded with 2 µL of the injectant.

The eggs were placed and oriented in the agar mold so that the cell in the fertilized egg (see Figure 8) was facing the microscope objective. The previously loaded needle was placed in the MM-3 Micromanipulator (*Narishige*) and oriented toward the egg. The microinjection pressure controller FemtoJet 4x (*Eppendorf*) was connected to the micromanipulator to ensure the injection. The injection pressure (pi) was set to 500-700 hPa and the compensation pressure (pc) was set to 80-100 hPa, with an injection time of 4 seconds. Due to the internal pressure of the medaka egg, the entire injection process must be finished within these 4 seconds. This includes pressing the injection pedal, inserting the needle in the egg, and then retracting the needle. Red color could be seen distributed in the cell cytoplasm if the injection was successful. The rest of the egg consists of egg yolk, and injection of this area would likely not edit the embryo unless some injectant was additionally dispersed in the cell.

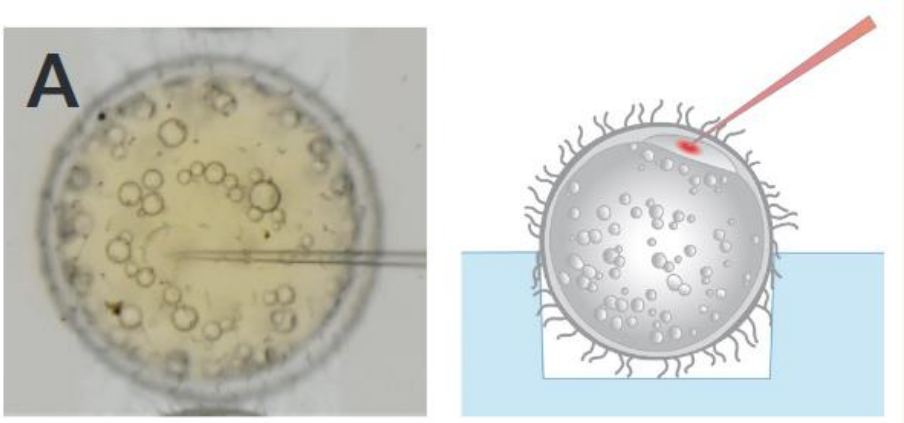

Figure 8: The microinjection needs to be done in stage one, before the developing cell divides. The cytoplasm of the first developing cell is surrounded by a bubble ring. Adapted from Thumberger et al. (62).

After injection, the eggs were collected and incubated at 28 °C in an embryo culture medium consisting of autoclaved system water supplied methylene blue, where the methylene blue would stain underdeveloped eggs which were removed. The embryo culture medium was changed daily upon hatching (which occurs at approximately 6-10 days). The injected eggs for the tg(*tshbb*:tdTomato) line were monitored in a microscope daily until hatching. Hatched larvae were then transferred to a 3.5-liter tank, housing 12 fish where they grew until adulthood after 2-3 months, making the founder generation.

2.5 Screening

2.5.1 DNA extraction

To screen the fish for the transgene, a DNA sample from an amputated caudal fin tip was taken. The fish were moved to a petri dish with system water supplied with 4% MS-222 Tricaine (*Pharmaq*) buffered with 8 g/L $NaHCO_3$ (*Pentair Aquatic Eco-Systems*) for anesthesia. A small piece of the fin was sampled with a clean scalpel blade. The fish was removed from the Tricaine solution as soon as possible after the amputation and put in an isolated 1-liter tank. It is important to isolate the individual fish and label the tank, for identifying the negative and positive individuals after genotyping results are obtained. The DNA was extracted with the Phire Animal Tissue Direct PCR Kit (*Thermo Fischer*), according to its supplied user guide. A small part of the caudal fin was removed with a scalpel as soon as the fish presented unconscious. The tissue was then submersed in 20 µL Dilution Buffer before 0.5 µL of DNARelease Additive was supplied. The sample was vortexed and spun down, went through cell lysis and DNA extraction, before being stored at -20 °C if not used immediately.

2.5.2 PCR

To confirm the successful integration of the transgene in the genome, PCR was performed on the extracted DNA from the clipped fin. Two different PCR protocols were tested and used for the different lines. Screening the tg(*tshbb*:tdTomato) line was challenging and several primers, annealing temperatures and PCR kits were tested. Suspicions of contamination of the negative DNA controls were disproved by several tests and led to discovering the specific PCR conditions successful in screening the tg(*tshbb*:tdTomato) line. The PCR kit for Taq

DNA Polymerase, recombinant (5 U/µL, *Thermo Scientific*) was used with a locally developed protocol for this line. The master mix consisted of 1 µL of 10 mM primer mix (see primers for *tshbb:tdTomato* in Table 3), 2.5 µL of 10X Taq Buffer with KCl, 2.5 µL of 25 mM MgCl2, 1 µL of a 10mM dNTP mix, 0.5 µL of 5 U/µL Taq DNA Polymerase and 17 µL of milli-Q water per sample in a 1.5 mL Eppendorf tube. 24 µL of the master mix was distributed in PCR strips per sample, and 1 µL of the extracted DNA samples was added to each tube in the strip. Water and WT medaka DNA were used as negative controls, while the vector plasmid was used as a positive control. The samples were run on the locally developed PCR program shown in Table 1 on the Veriti 96 Well Thermal Cycler (*Thermo* Fischer).

Table 1: PCR program used for screening the tg(tshbb:tdTomato) line

Step	Temperature	Time	Cycles
Initial Denaturation	94 °C	3 minutes	1 Cycle
Denaturation	94 °C	45 seconds	35 Cycles
Annealing	55 °C *	30 seconds	
Extention	72 °C	90 seconds/kb	
Final Extension	72 °C	10 minutes	1 Cycle
Hold	4 °C	Indefinitely	

For screening the tg(*fshb*:NTR-CFP/*fshb*:DsRed2) line the kit Phire Hot Start II DNA Polymerase (*Thermo Fischer*) was used. The master mix and samples were prepared according to the manufacturer's recommendations. Water and WT medaka DNA were used as negative controls, while the vector plasmid was used as a positive control. The samples were run on the kit 3-step PCR program shown in Table 2 on the Veriti 96 Well Thermal Cycler.

Table 2: PCR program used for screening the tg(fshb:NTR-CFP/fshb:DsRed2) line

Step	Temperature	Time	Cycles
Initial Denaturation	98 °C	30 seconds	1 Cycle
Denaturation	98 °C	5 seconds	35 Cycles
Annealing	60 °C	5 seconds	
Extention	72 °C	10-15 seconds/kb	
Final Extension	72 °C	1 minute	1 Cycle
Hold	4 °C	Indefinitely	

Table 3: Primers used for screening the DNA samples from the transgenic medaka

Primer name	Forward sequence 5'-3	Reverse sequence 5'-3'	Amplicon length (bp)
nfsB	GCGTCATTCCACTAAGGCAT	GCGGCCGCTTACACTTCGGTTAAGGTGATGTTTTG	634
tshbb:tdTomato	GCGGCAGAATTTGGTTGTAT	GCCATGCCCCAGGAACAG	854

When the PCR program was finished, the samples were run on gel electrophoresis to visualize the results. 1% Agarose gel is prepared by dissolving 1 g of Electran Agarose DNA Grade (*VWR Chemicals*) per 100 mL of 1X Tris-acetate-EDTA (TAE) buffer. 3 µL of SYBR Safe DNA Gel Stain (*Thermo Scientific*) per 100 mL gel was added to enable visualization of DNA. The gel was set to solidify in a gel- and well-mold while being shielded from light for approximately 20-30 minutes or thoroughly solid. Meanwhile, the PCR samples received Gel Loading Dye (6X) (*Thermo Scientific*) diluted 1:5, to weigh down the DNA samples in the sample wells. The gel was applied to the electrophoresis chamber supplied with the TAE buffer before 5 µL of the Gene Ruler 1k (*Thermo Scientific*) was added in 2-3 wells evenly distributed in the gel. 10 µL of the dyed samples was added to the remaining wells. The gel was run at a current of 110 V for approximately 30-40 minutes in the Model 200/2.0 Power Supple electrophoresis chamber (*Bio-Rad*) and pictured with GenoSmart (*VWR*) and the transilluminator Safe Imager (*Invitrogen*), illuminating the DNA bands. Positive and negative samples could then be distinguished based on the presence of bands and expected amplicon length shown in Table 3.

2.6 Breeding program

After screening the animals, negative fish were euthanized, while the injected fish positive for the transgene were selected to be founders of the transgenic line (generation F0). Injected founder fish most likely carry one copy of the transgene, making them hemizygous carriers (63). Transgenic lines are made by breeding the fish for their transgene (see Table 4).

One F0 fish (genotype T) and one WT fish (genotype tt) of each sex were coupled together (T x tt) in a 1-liter aquarium tank to produce F1 eggs. These eggs were collected from the female, and the egg filaments were removed. They were kept at 28 °C in an incubator in a Petri dish with embryo culture medium changed daily until hatching. Upon hatching at

approximately 6-10 dpf, the F1 larvae were transported to a 3.5-liter aquarium in groups of 12 individuals, where they grew until adulthood in approximately 2-3 months. This F1 generation was screened by genotyping, as described for the F0 generation. The positive heterozygous F1 fish are intercrossed (Tt x Tt) with each other to start creating a stable transgenic line.

Furthermore, the plan was to create the F2 generation. However, because of time limitations, this remains to be done. The crossing of 2 fish from the F1 generation will produce the F2 generation composed of a heterozygous (Tt) and homozygous (TT) mixture of transgene-positive fish. F2 fish would in turn be crossed with WT fish (Tt x tt or TT x tt) to produce eggs. The eggs will be screened with PCR to determine if the F2 parents were homozygous or heterozygous for the transgene, depending on the ratio of positive offspring. 0% positive eggs, means they are negative, or unable to pass on the transgene. The parents will be considered heterozygous if 50% of their eggs are positive while considered homozygous if 90-100% of their eggs are positive. Homozygous F2 fish will be intercrossed to produce a stable homozygous line.

Table 4: Schematic representation of the passing of the transgene in the breeding program (chromosomes are T = positive, or t = negative for the transgene). Wildtype medaka are homozygous negative for the transgene (tt), while F0 fish are hemizygous (T) and carry only one allele of the transgene. Positive F1 fish are heterozygous (Tt), while positive F2 fish are homozygous (TT) or heterozygous (Tt).

Male\Female	**tt**	**T**	**Tt**	**TT**
tt	tt tt tt tt	Tt Tt t t	Tt Tt tt tt	Tt Tt Tt Tt
T	Tt Tt t t			
Tt	TT Tt Tt tt		TT Tt Tt tt	TT TT Tt Tt
TT	Tt Tt Tt Tt		TT TT Tt Tt	TT TT TT TT

2.7 Ex vivo pituitary tissue culture

To dissect the brain- and pituitary tissue, the fish were euthanized by an overdose of 10% Tricaine. Once unconscious, the dissection was performed according to this paper by Fontaine et al. (64). Here, the pituitary was present as a small purple gland on the ventral side of the revealed brain. The pituitary is loosely attached to the brain and should be watched carefully to not lose it. The tissue was temporarily stored in ice-cold Dulbecco's phosphate-buffered saline (dPBS) before being transferred to medaka tissue culture. The dPBS was adjusted to pH 7.75 with HCl or NaOH and an osmolarity of 290 mOsm/kg with D-Mannitol (*Sigma-Aldrich*) before sterile filtering.

Three different medaka tissue cultures (Table 5) were prepared and tested on BP tissue from wildtype fish. The first (Culture 1) by Karigo et al. (65), the second (Culture 2) by Ager-Wick et al. (66), and a third locally developed mix of these two preparations (Culture 3).

Table 5: Compositions of the three tested tissue cultures

	Culture 1	**Culture 2**	**Culture 3**
Leibovitz's L-15 culture medium (pH 7.4) [*Sigma-Aldrich*]	500 mL	500 mL	500 mL
2 mM Glutamax Supplement (L-Glutamine) [*Thermo Fischer*]	5 mL	5 mL	5 mL
10 mM D-Glucose [*Sigma-Aldrich*]	0.9 g	0.4 g	0.9 g
5% Fetal Bovine Serum [*JRH Biosciences*]	25 mL	-	25 mL
10 mM $NaHCO_3$ [*Sigma-Aldrich*]	-	5.6 mL	5.6 mL
Sterile-filter [*Santa Cruz Biotechnology*]	Yes	Yes	Yes
Penicillin-Streptomycin [*Thermo Fischer*]	2.5 mL (Must be added after sterile-filtering)	2.5 mL (Must be added after sterile-filtering)	2.5 mL (Must be added after sterile-filtering)

These three tissue cultures were tested in incubator conditions with (1%) and without (0%) CO_2 supplementation to determine the ultimate environment for keeping pituitary tissue (Figure 9). This was investigated because the L-15 Culture medium was originally developed to not require CO_2 gas supplementation (67). Two brains were dissected per medium and kept in a well each in the TC Plate 24 Well, Cell+, F (*Sarstedt*) for 8 days in the incubator at 26 °C. The tissue was checked daily for parameters like the pH indicator color of the culture, amount of tissue debris in the medium, contamination, and general degradation of the tissue. To determine how healthy the tissue stayed in the tested conditions, the increase of observed tissue debris was compared to fresh tissue with no debris. The quantity of tissue debris was scored on a scale from 0 to 5 (0 = no increase, 5 = complete degradation) and converted into percentage (5 = 100%). The culture medium was replaced and scored on days 1 to 5 and additionally scored on day 8.

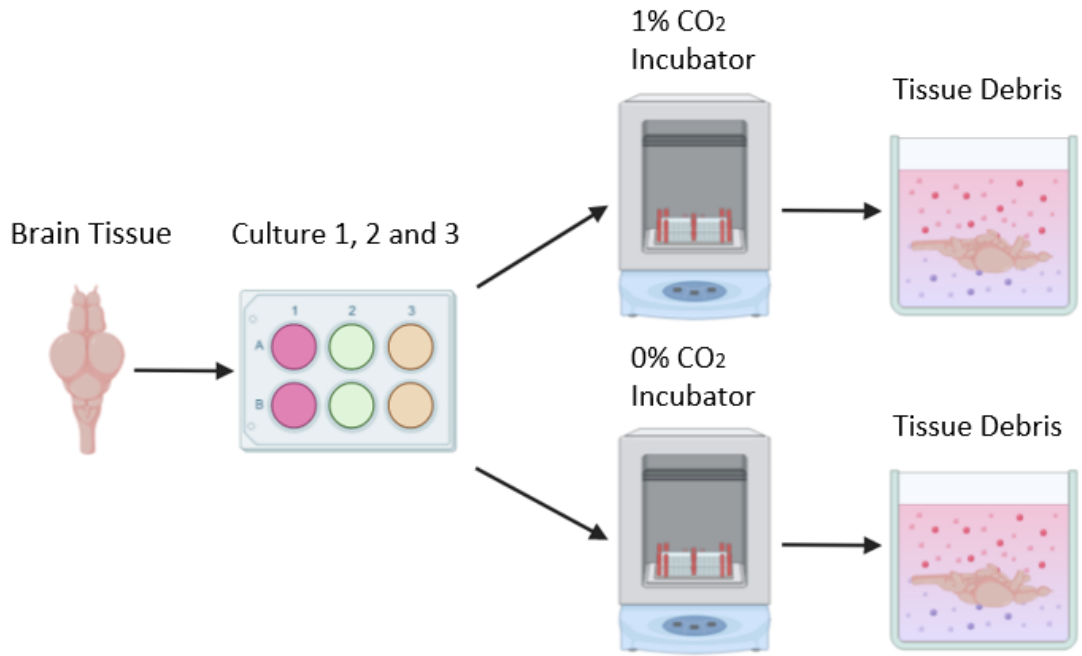

Figure 9: Simplified illustration of how the tissue cultures and the ideal conditions were tested. Brain tissue was stored in Culture 1, 2 and 3, and kept in two different CO_2 concentrations. The degradation of the brain tissue was determined by observing the daily increase of tissue debris in the culture medium (Made in Biorender ©).

When the best medium and conditions were determined, the effect of RZ on ex vivo brain- and pituitary tissue from positive tg(*fshb*:NTR-CFP/*fshb*:DsRed2) line was tested. The concentrations of 10 mM, 50 mM, and 100 mM Ronidazole (*Sigma-Aldrich*) were tested to find the most effective and least lethal dosage of the treatment to ablate the Fsh cells.

Dissected brain- with pituitary tissue were incubated in the different concentrations of RZ in the tissue culture medium supplied with 1% dimethyl sulfoxide (DMSO) in the well-plate before being maintained in the incubator at 26 °C (with and without CO_2 supplementation). In all the treatments, the culture medium was changed daily on days 1 to 5.

The RZ treatments lasted for 8 days, where RZ was supplied at every medium change in the 10 mM treatment. For the 50 mM treatment RZ was supplied on day 1 and 2, and only on day 1 for the 100 mM treatment. The fluorescence reduction of CFP and RFP was observed and compared to the fluorescence intensity on Day 1 of treatment. The fluorescence reduction determined how effectively the RZ treatment ablated the Fsh cells. The fluorescence was scored on a scale from 0 to 5 (0 = no decrease, 5 = total decrease to no fluorescence) and converted to percentage (5 = 100%). The fluorescence was scored for days 1 to 5 and on day 8. Tissue debris quantity was also monitored, as previously described.

2.8 Tissue sectioning

To verify co-expression of the fluorescent reporter proteins, and the potential RZ-driven ablation of the Fsh cells, tissue slices were made. Confirmation of the presence of CFP and RFP was first made with fluorescent microscopy, before treating the cells with RZ for 24 hours. After treatment, the tissue was moved to dPBS and then fixated in 4% paraformaldehyde (PFA; *Electron Microscopy Sciences)* diluted in PBS-Tween (PBST) for at least 24 hours at 4 °C.

After fixation, the tissue was washed twice in PBS for 5 minutes. It was then oriented in a plastic mold and embedded in 3% agarose (diluted in ddH_2O) before being left to solidify for 5 minutes at room temperature. Excess agarose was trimmed with a clean scalpel blade from the block containing the tissue, and the block was immersed in PBST. The tissue was parasagittally sectioned at 60 μm thickness using the vibratome VT1000 S (*Leica*).

To confirm the viability of the tissue after the RZ treatment, the tissue sections were treated with 4′,6-diamidino-2-phenylindole (DAPI). A DAPI stain illuminates DNA, visualizing

living cells under UV light by examining the morphology of the nucleus. Living cells usually have a smooth round cell membrane and nucleus, whereas apoptotic cells create apoptotic bodies (a process called blebbing) containing cellular contents with or without DNA fragments. Due to an increased permeability of apoptotic bodies, DAPI strongly stains the DNA fragments in apoptotic cells which makes apoptotic bodies highly detectable (68). These morphological differences make it possible to confirm the potential toxicity of high RZ concentrations to the tissue. Tissue slices were temporarily placed carefully in filter containers filled with PBST. The PBST was removed, and excess moisture was removed with clean paper. The slices were treated with DAPI (4′,6-diamidino-2-phenylindole; 300 nM, *Sigma-Aldrich)* for 30 minutes protected from light, before being transferred to a Petri dish containing PBST by pipetting the buffer under the filter. The tissue was then collected on a microscopy slide, and excess moisture was carefully removed with clean paper. The tissue was then covered in Vectashield Antifade Mounting Medium (*Vector Laboratories*) and a glass cover slip.

2.9 Imaging

2.9.1 Tracing egg development

F0 and F1 eggs for the tg(*tshbb*:tdTomato) line were monitored daily until hatching using a Nikon Stereo Microscope (SMZ25, *Nikon*) with the SHR Plan Apo 1x WD:60 objective. The eggs were imaged with white light and filters for tdTomato (excitation/emission: 554 nm/581 nm). The images were obtained at different magnifications ranging from 1x to 8x to observe the potential appearance of the *tshbb* expression between 0 dpf and 10 dpf (pre-hatching). Eggs from the tg(*fshb*:NTR-CFP/*fshb*:DsRed2) line were not imaged, since expression of *fshb*:DsRed2 fluorescence has been shown to barely be visible before 1 month post fertilization in the pituitary (38).

2.9.2 Tissue imaging

Dissected brain- and pituitary tissue from adult medaka from the tg(*fshb*:NTR-CFP/*fshb*:DsRed2) line was tested in different tissue cultures and CO_2 environments before being treated with RZ. When testing the ideal conditions for the tissue, the Nikon Stereo Microscope was used with white light imaging at 1x and 2x magnification to show potential

tissue degradation. Pictures were taken on days 1 to 5 (in addition to day 8) post-dissection for comparing the three different tissue cultures and two different CO_2 environments.

When the ideal conditions were determined, the tissue was treated with RZ and monitored from days 1 to 5 (in addition to day 8). Here, the tissue was imaged with the Nikon Stereo Microscope with white LED light, with filters for CFP (excitation/emission wavelengths: 484 nm/510 nm) and DsRed2 (excitation/emission wavelengths: 563 nm/582 nm) (69). It is worth noting that this microscope did not have a CFP filter, and the GFP filter was used instead since the excitation and emission specters overlap, which allows observation of CFP expression (70). For consistency, the images were taken at 3x magnification for all wavelengths, with an exposure time of 300 milliseconds for the detection of the fluorescence markers.

To verify the co-expression of *fshb:*NTR-CFP and *fshb*:DsRed2 in the same cells, and their potential ablation, the pituitary tissue was imaged before and 24 hours after RZ treatments. The tissue was, as previously mentioned, sectioned, before being imaged on the DM6 B Upright Microscope (DM6 B, *Leica*) with 20x/0.8 and 63x/1.4 HC Plan Apochromat objectives. Imaging was done with white light, and emission lasers for DAPI (405 nm), CFP (550 nm), and DsRed2 (590 nm) at 20x and 63x magnification. The images were processed with the microscope software Leica Application Suite X and ImageJ from Fiji (71).

2.10 Statistics

A two-way ANOVA with Tukey’s multiple comparison test was used to compare the mean quantity of tissue debris between the three different tissue culture mediums in the different CO_2 concentrations. A two-way ANOVA with Šídák's multiple comparison test was used to compare the tissue degeneration overall, in the different tissue culture mediums, and between two specific culture mediums in 1% CO2 and 0% CO2 conditions. To do this, the software GraphPad Prism 10 (*GraphPad Software*) was used. The statistical significance was set to $P < 0.05$. Statistical tests were not performed in other experiments due to the limited number of replicates.

3. Results

3.1 Generation of tg(*tshbb*:tdTomato)

3.1.1 Specific PCR conditions

To screen the tg(*tshbb*:tdTomato) line, 12 different primer sets, 6 different annealing temperatures and 2 different PCR kits were tested. While many of the primer sets failed to amplify any sequences or samples. Several sets of primers successfully amplified the *tdTomato* transgene in the positive plasmid control but also showed false positives with bands around the expected size. The amplified bands were of and unknown DNA sequence in the negative WT control DNA as depicted in Figure 10 when using the PCR kit Phire Hot Start II DNA Polymerase (*Thermo Fischer*). Contamination was disproved in the water, DNA extraction reagents, PCR reagents and in the gel electrophoresis process.

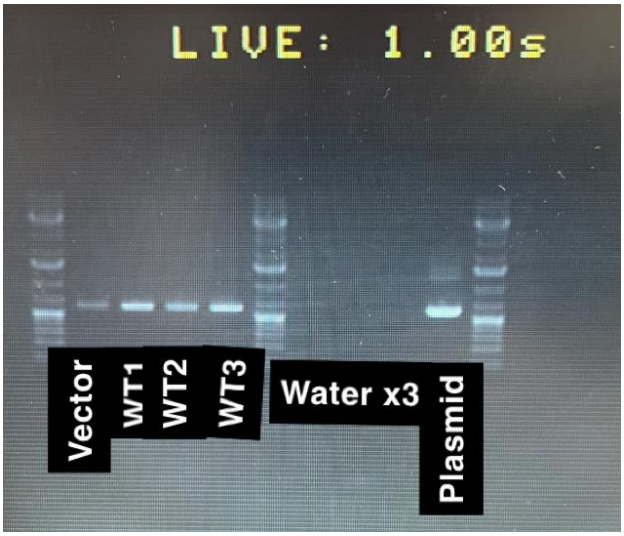

Figure 10: PCR results depicting wildtype (WT) DNA positive for tdTomato at approximately 600 bp (Relevant 1kb Plus GeneRuler brightests band sizes from bottom: 500 bp, 1500 bp).

Successful screening of this line was first achieved when testing one of the previous primer sets on the PCR kit for Taq DNA Polymerase, recombinant (5 U/µL, Thermo Scientific). This primer combination annealed to both the *tshbb* and *tdTomato* sequences, whereas previous primer sets were designed for only the *tdTomato* sequence. The successful primers are depicted in Table 3, and the PCR program in Table 1.

3.1.2 F0

Of the injected eggs of the tg(*tshbb*:tdTomato) line, 70 eggs grew up to adulthood (Table 6), while being monitored throughout the egg development. The only fluorescence observed was due to the auto-fluorescence of the egg yolk or the skin pigmentation of the larvae. 1/50 (2%) fish screened positive for the *tdTomato* sequence with PCR (Table 6). Here, negative individuals had 1 band at 300 bp – 400 bp (not present in the plasmid control), while an additional band of 854 bp was expected for positive transgenic fish (matching the positive plasmid control) as shown in Figure 11.

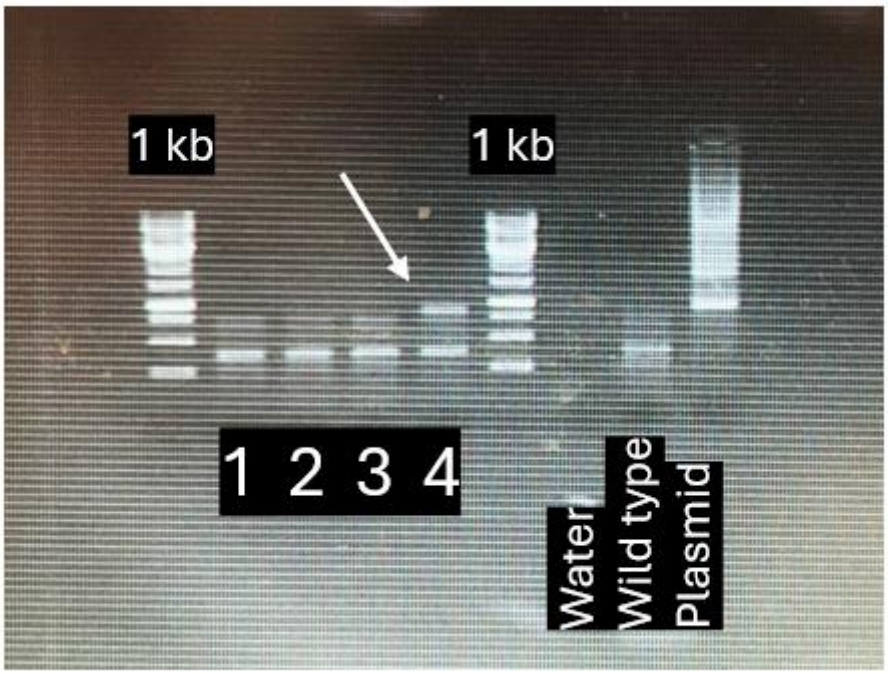

Figure 11: Example of PCR results when screening the tg(tshbb:tdTomato) line. Numbers 1-4 indicate 4 different fish, where the arrow shows an additional band in fish number 4, making it positive for tdTomato. Water and wildtype DNA were used as negative controls, and the injectant plasmid tshbb:tdTomato as a positive control (Relevant 1kb GeneRuler band sizes from bottom: 250 bp, 500 bp, 750 bp, 1000 bp).

3.1.3 F1

This positive male founder fish (F0) was coupled with two WT females, for one week per female to produce the F1 eggs. 84 F1 eggs were collected from the first WT female, and 91 F1 eggs were collected from the second WT female (Table 6). These eggs were monitored daily under the microscope.

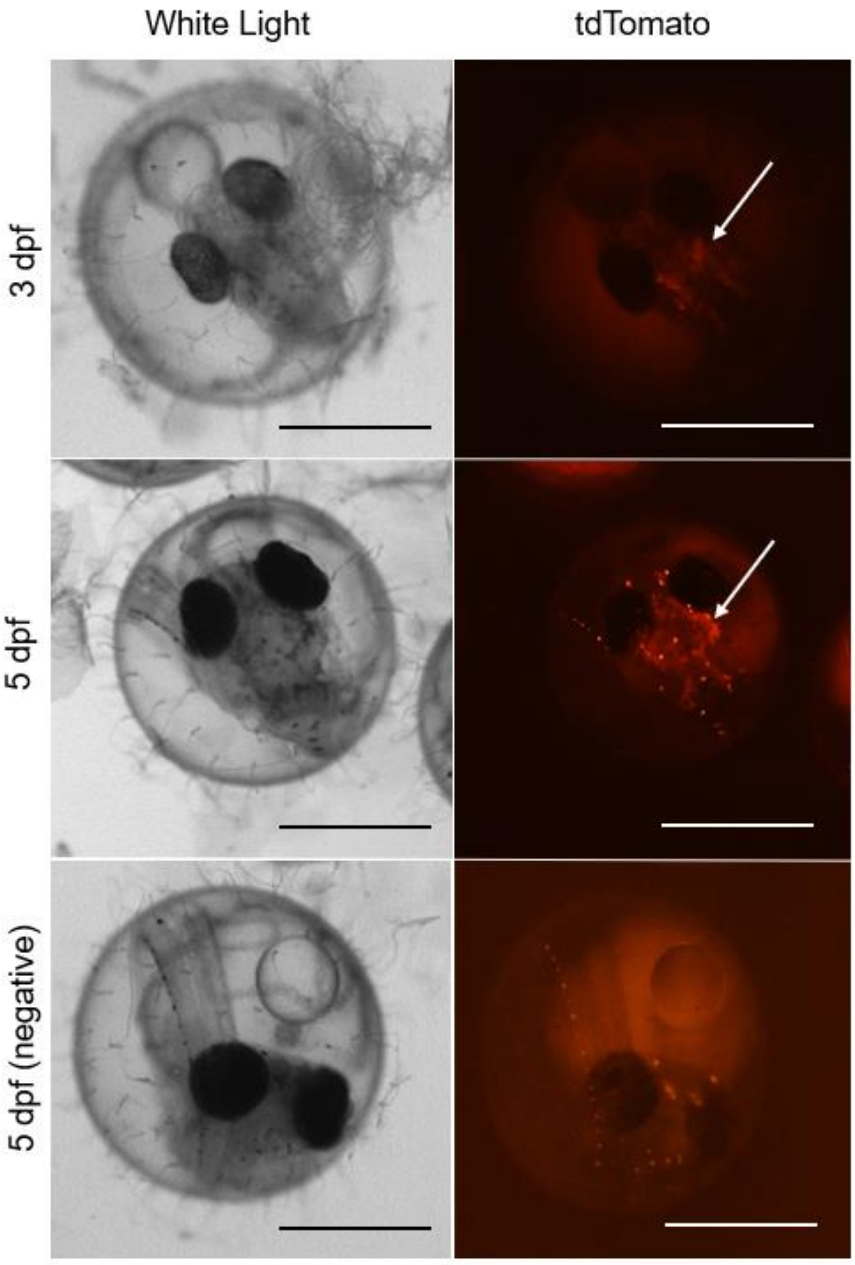

Figure 12: Fluorescent imaging of medaka larvae. From 3 days post fertilization a group of fluorescent cells (white arrow) emerged in F1 larvae. A larva without this cell population is shown in the bottom panel. (Magnification: 4x, zoomed in; Scale bars = 500 µm).

Only auto-fluorescence was seen before 3 dpf (Figure 12) when a group of fluorescent cells emerged between the eyes in many F1 larvae. This cell population stayed visible until hatching at 8 dpf, where the larvae were left to grow until adulthood. Unfortunately, because of time limitations, the F1 generation remains to be screened with PCR, and positive fish to be found before intercrossing them.

Table 6: Number of collected eggs that reached adulthood, screened individuals, and number of positive fish for the tg(tshbb:tdTomato) line

Generation	Matured eggs (n)	Individuals screened	Positive (n)	Positivity percentage (%)
F0	70	50	1	2
F1	175	0	*NA*	*NA*

3.2 Generation and tissue analysis of tg(*fshb*:NTR-CFP/*fshb*:DsRed2)

3.2.1 F1

Injected F0 fish were previously screened in the laboratory. The positive fish were crossed with WT to produce F1 eggs. 76 F1 eggs were collected and raised until adulthood. When screening with PCR, 38 fish (50%) were positive for *nfsB.* Negative individuals had no band, while positive fish showed a band of 634 bp (see Figure 13). Couples of positive fish were intercrossed (F1 x F1).

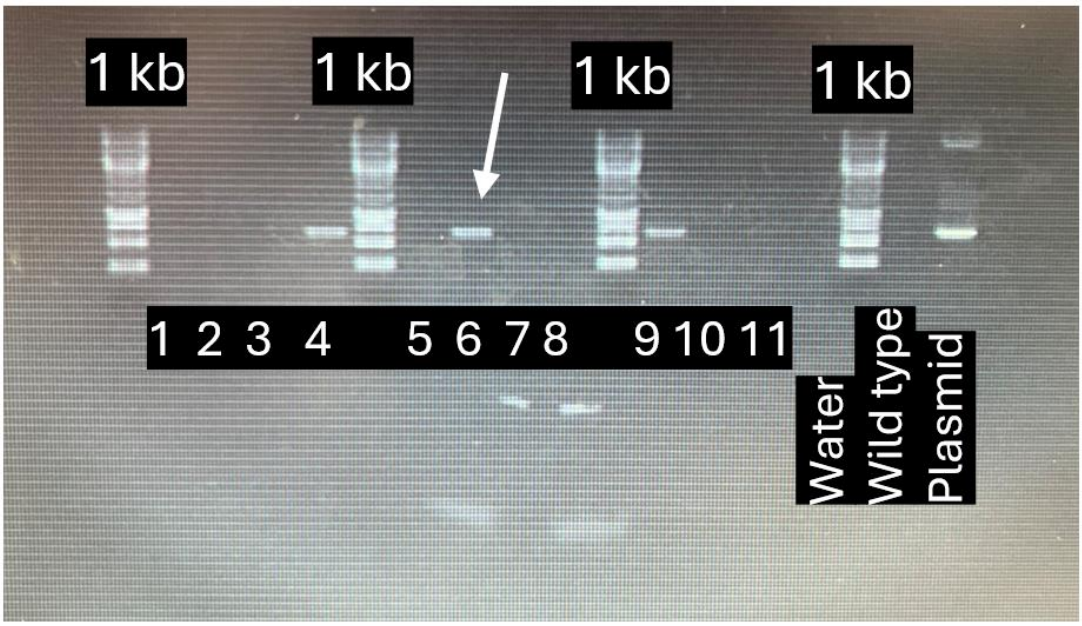

Figure 13: Example of PCR results when screening the tg(fshb:NTR-CFP/fshb:DsRed2) line. Numbers 1-11 indicate 11 different fish, where the arrow shows a fish positive for nfsB. Water and wildtype DNA were used as negative controls, and the injectant plasmid fshb:NTR-CFP as a positive control (Relevant 1kb GeneRuler band sizes from bottom: 250 bp, 500 bp, 750 bp).

3.2.2 F2

113 F2 eggs were collected from the F1 x F1 couples and raised until adulthood (Table 7). 20 of these fish were screened with PCR, where 13 (65%) were positive for *nfsB*. Unfortunately, because of time limitations, the rest of the F2 generation remains to be genotyped.

Table 7: Number of collected eggs that reached adulthood, screened individuals, and number of positive fish for tg(fshb:NTR-CFP/fshb:DsRed2)

Generation	Matured eggs (n)	Individuals screened (n)	Positive (n)	Positivity percentage (%)
F1	76	76	38	50
F2	113	20	13	65

3.2.3 Tissue culture and condition testing

When testing the different tissue culture mediums for the ex vivo brain- and pituitary experiments, fish negative for the transgene and WT fish were used in the experiments. The daily amount of tissue debris over 8 days was compared to debris-free tissue culture from day 1. The three tissue cultures were also compared in two different incubator conditions, 1% CO_2 and 0% CO_2 (Figure 14).

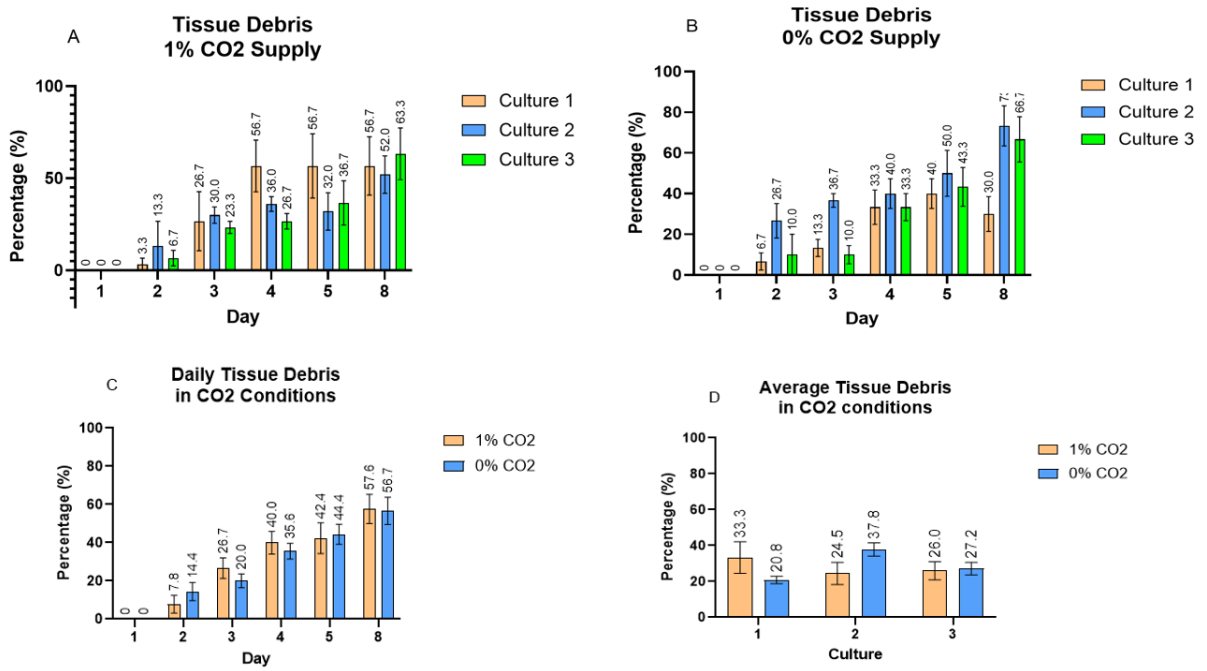

Figure 14: Comparison of average tissue debris increase with 1% CO_2 and 0% CO_2 over 8 days. The percentage of daily generation of tissue debris in (A) 1% CO_2 and (B) 0% CO_2 conditions (Culture 1 = orange, Culture 2 = blue, Culture 3 = green; n = 6). C) Comparison of daily tissue debris generation for all cultures in 1% CO_2 and 0% CO_2 conditions (1% CO_2 = orange, 0% CO_2 = blue; n = 18). D) Comparison of average tissue debris generation for cultures in 1% CO_2 and 0% CO_2 conditions (1% CO_2 = orange, 0% CO_2 = blue; n = 6). (Error bars (± SEM) are shown as black bars in the graphs).

When comparing the daily tissue debris for the tissue cultures kept in 1% CO_2 (n = 6), no significant difference was found between any of the cultures, as seen in

Table 8 (P > 0.05). The pH indicator of the mediums showed that Culture 1 slightly decreased in pH, while Cultures 2 and 3 remained stable after 24 hours (*data not shown*). When comparing the tissue debris of the cultures in 0% CO_2 (n = 6), there was, however, a significant difference between Culture 1 and Culture 2 on day 3 ($p = 0.0043$), Culture 2 and Culture 3 on day 3 ($p = 0,0024$), and Culture 1 and Culture 2 on day 8 ($p = 0.0201$). The difference between Culture 1 and Culture 3 on day 8 was also close to significance ($p = 0.0649$). This shows that on the 3rd day, Culture 2 showed a significantly higher generation of tissue debris compared to the other cultures. Additionally, Culture 1 generated significantly less tissue debris than Culture 2 (and nearly significantly lower than Culture 3) on the 8th day. The pH indicator of the mediums showed that Culture 1 slightly decreased in pH, while Cultures 2 and 3 increased after 24 hours (*data not shown*).

Table 8: Two-way ANOVA with Tukey's Multiple Comparison. P-values are shown for tissue cultures in 1% and 0% CO_2 concentrations. Significant values are marked in bold, and values close to significance in italics (Significance threshold P < 0.05).

	p-values (1% CO_2)					**p-values (0% CO_2)**				
Day	2	3	4	5	8	2	3	4	5	8
Culture 1 vs. Culture 2	0.7578	0.9783	0.3944	0.4754	0.9669	0.1517	**0.0043**	0.8246	0.7442	**0.0201**
Culture 1 vs. Culture 3	0.8128	0.9776	0.1840	0.6281	0.9472	0.9497	0.8526	>0.9999	0.9587	*0.0649*
Culture 2 vs. Culture 3	0.8845	0.4842	0.2924	0.9531	0.7959	0.4409	**0.0024**	0.7833	0.8948	0.8967

Data for all tissue cultures in 1% CO_2 and 0% CO_2 were pooled and compared (Table 9) to detect any differences between the CO_2 conditions (n = 18). No significant differences in tissue debris amount were found for any of the days. Lastly, the culture medium variants were compared between the two CO_2 conditions (n =6), with no significant differences detected.

Table 9: Two-way ANOVA with Šídák's Multiple Comparisons Test. P-values are shown for daily comparison between all tissue cultures (left) and culture average (right) in 1% CO_2 and 0% CO_2 (Significance threshold P < 0.05).

	p-values (1% CO_2 vs. 0% CO_2)		
Day	**Daily average**	**Culture**	**Weekly average**
2	0.9042	**1**	0.1203
3	0.8930	**2**	0.0993
4	0.9910		
5	>0.9999	**3**	0.8799
8	>0.9999		

For further notice, the 10 mM RZ treatment was performed in Culture 3 (1% CO_2), while the 50 mM and 100 mM were done in Culture 1 (0% CO_2). These two culture conditions were therefore compared (without RZ supplementation) to detect their potential impact on tissue health (Figure 15).

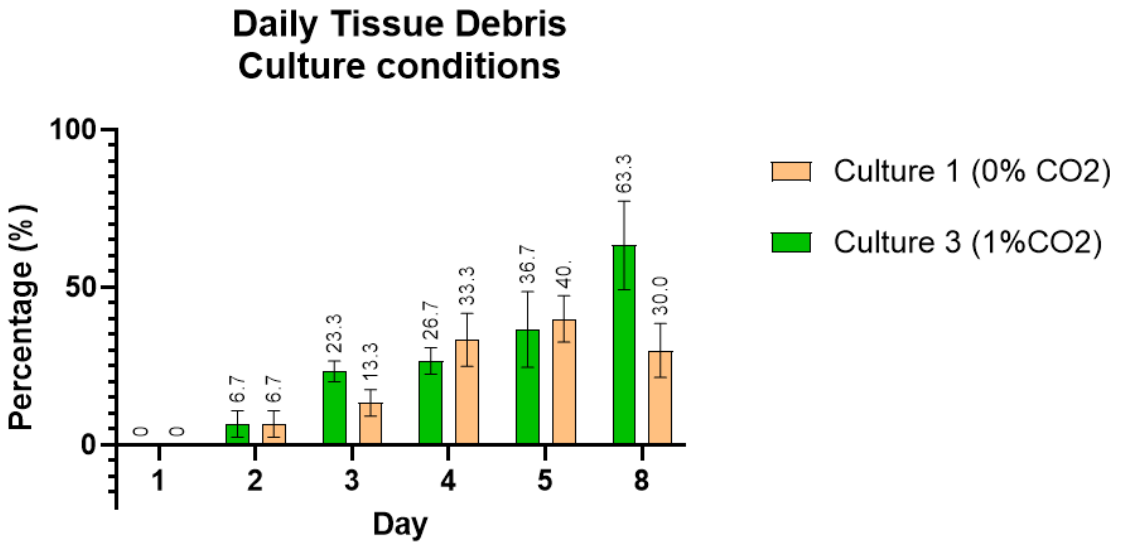

Figure 15: Comparison of daily tissue debris generation between Culture 1 (0% CO2) and Culture 3 (1% CO2) (Culture 1 = orange, Culture 3 = green; n = 6).

The test revealed no significant differences in tissue degeneration from days 1 to 5 (Table 10). On the 8th day of the experiment, there was however a significant difference between the culture conditions ($p = 0.0106$).

Table 10: Two-way ANOVA with Šídák's Multiple Comparisons Test. P-values are shown for daily comparison between Culture 1 in 0% CO_2 and Culture 3 in 0% CO_2. Significant values are depicted in bold. (Significance threshold $P < 0.05$).

Day	p-values (Culture 1 (0% CO2) vs. Culture 3 (1% CO2))
2	>0.9999
3	0.9096
4	0.9870
5	0.9997
8	**0.0106**

To conclude, no significant difference was found between the tissue cultures with 1% CO_2. In the tissue cultures with 0% CO_2, Culture 2 had significantly higher debris generation than Cultures 1 and 3 at day 3, and Culture 1 at day 8. Additionally, Culture 1 showed a (close to significantly) lower degree of tissue debris than Culture 3. This suggested that Culture 2 should not be recommended for 0% CO_2 conditions. There was no significant difference in overall daily tissue debris generation between CO2 conditions. There was also no significant

difference in average tissue degradation between the culture mediums in different CO_2 concentrations. There was however a significant difference in how long the tissue remained healthy between specific culture conditions. Culture 1 (0% CO2) seemed preferrable for longevity of tissue health when kept in culture medium.

3.2.4 Ablation of Fsh cells with Ronidazole

Dissected pituitaries were treated with 0 mM and 10 mM RZ, to confirm the possibility for ablation of the Fsh cells. Two *nfsB*-positive pituitaries were kept in Culture 3 (1% CO_2) for 24 hours; one in 0 mM RZ supplementation, and one in 10 mM RZ. First, fluorescence intensity was confirmed before and after treatment (Figure 16 and Figure 18B). Second, CFP- and DsRed2 were localized in the same positions in the pituitary, confirming the expression of NTR in Fsh cells (Figure 17: Top panel).

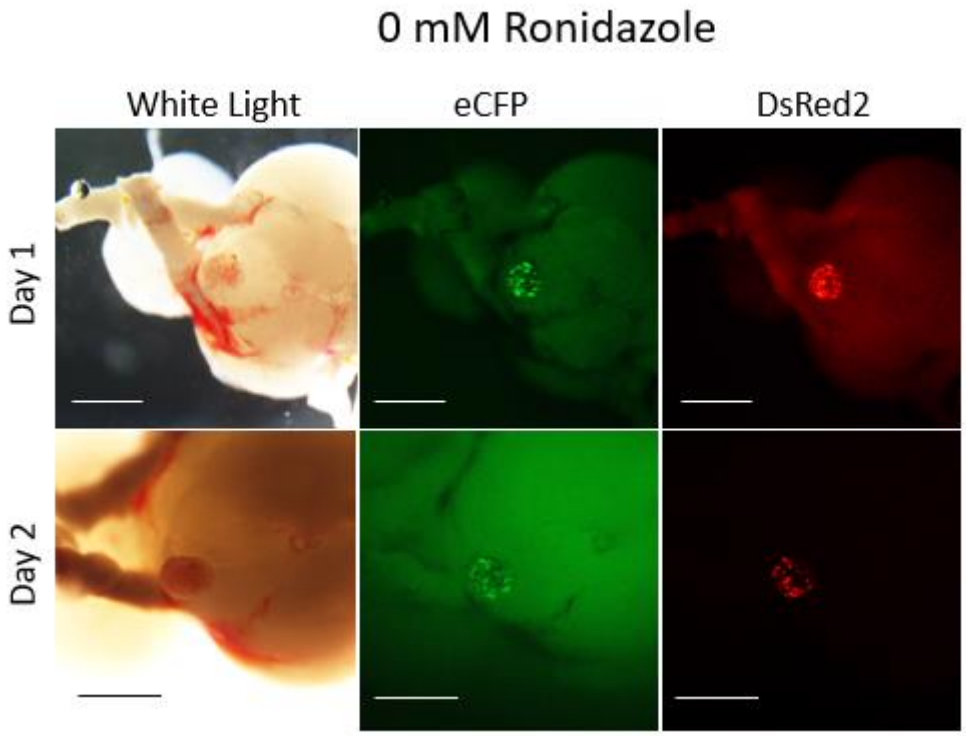

Figure 16: Imaged pituitary (oriented anterior to the left, posterior to the right) at days 1 and 2 of 0 mM ronidazole treatment (Magnification 2x; Scale bars = 1 mm).

Finally, when observing the pituitary treated with 10 mM RZ, it was confirmed that CFP intensity was greatly reduced, while still strongly expressing DsRed2 (Figure 17: Bottom panel).

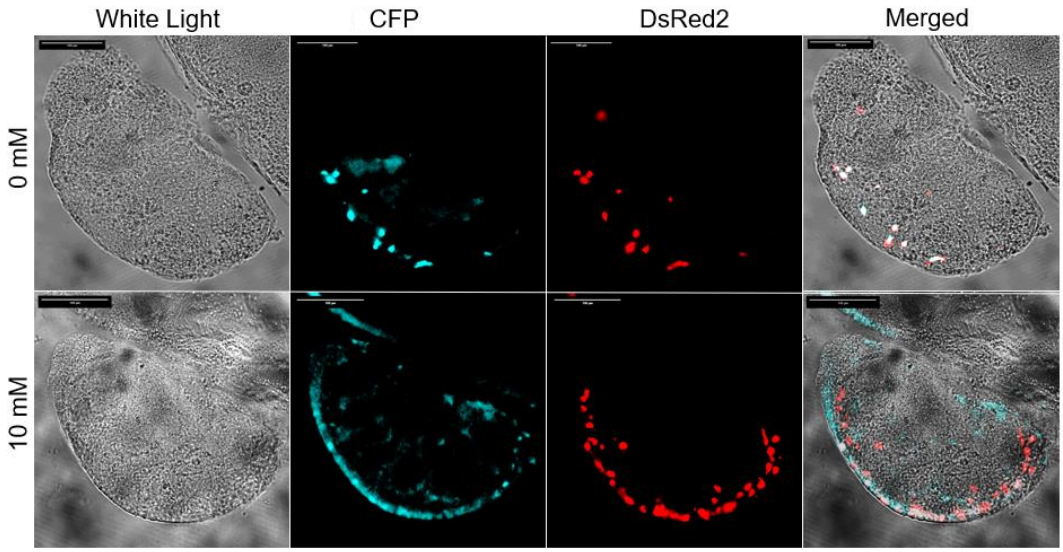

Figure 17: Sliced pituitary before and after treatment of 0 mM and 10 mM ronidazole (oriented anterior to the left, posterior to the right). Top panel: Co-expression of CFP (blue) and DsRed2 (red) co-expressing in the same cells (white, in the far right image) Bottom panel: Few cells with solid CFP expression were identified, while still showing weak fluorescence along the anterior and ventral side. DsRed2 was, still fluorescent post-treatment with 10 mM ronidazole. The far right image shows few co-expressing cells in white (Magnification 20X; Scale bars = 100 μm).

Based on the previous statistical tests, the RZ treatments were performed in two different conditions, due to new discoveries about the culture mediums during the project. First, Culture 3 (1% CO_2) was used for the 10 mM RZ treatment. This was later changed to Culture 1 (0% CO_2) for the 50 mM and 100 mM RZ treatments. Dissected brain- and pituitary tissue from *nfsB*-positive F1 and F2 adult fish were tested for 8 days.

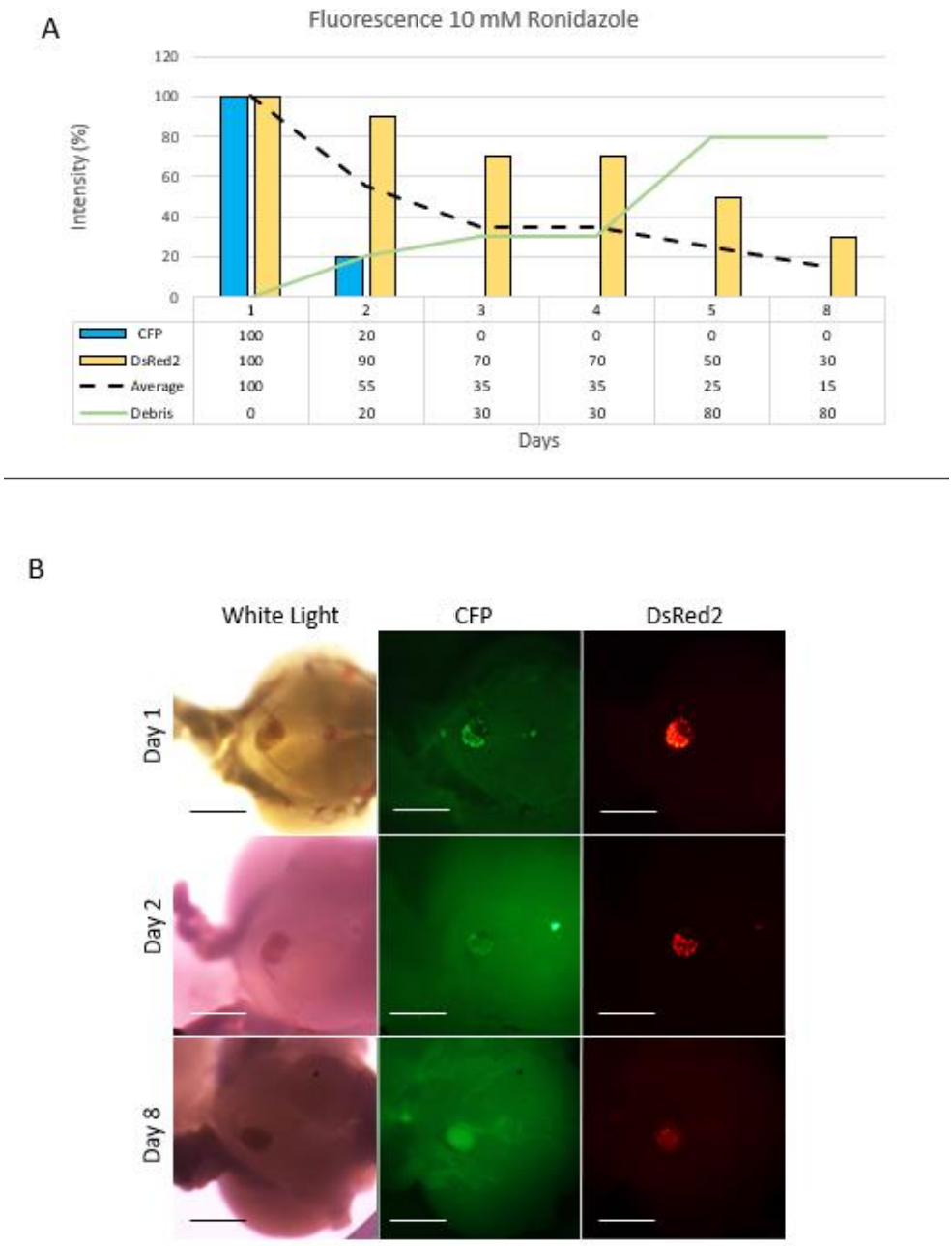

Figure 18: Fluorescence intensity monitoring of nfsB positive pituitary over 8 days in 10 mM ronidazole treatment. A) Fluorescence intensity of CFP (blue), DsRed2 (orange), average fluorescence (black) and amount of tissue debris (green) (n = 1). B) Imaged pituitary (oriented anterior to the left, posterior to the right) at days 1, 2 and 8 in white light, CFP (green) and DsRed2 (red) (Magnification 2x; Scale bars = 1 mm).

When treating the tissue with 10 mM RZ for 8 days, both CFP and DsRed2 were monitored (Figure 18). CFP intensity decreased from 100% on day 1 to 20% on day 2. The fluorescence was undetectable by day 3 and did not recover towards the end of the experiment. The fluorescence intensity of DsRed2 remained at 30% until the 8th experiment. The amount of tissue debris increased steadily throughout the experiment, reaching 80% at day 8.

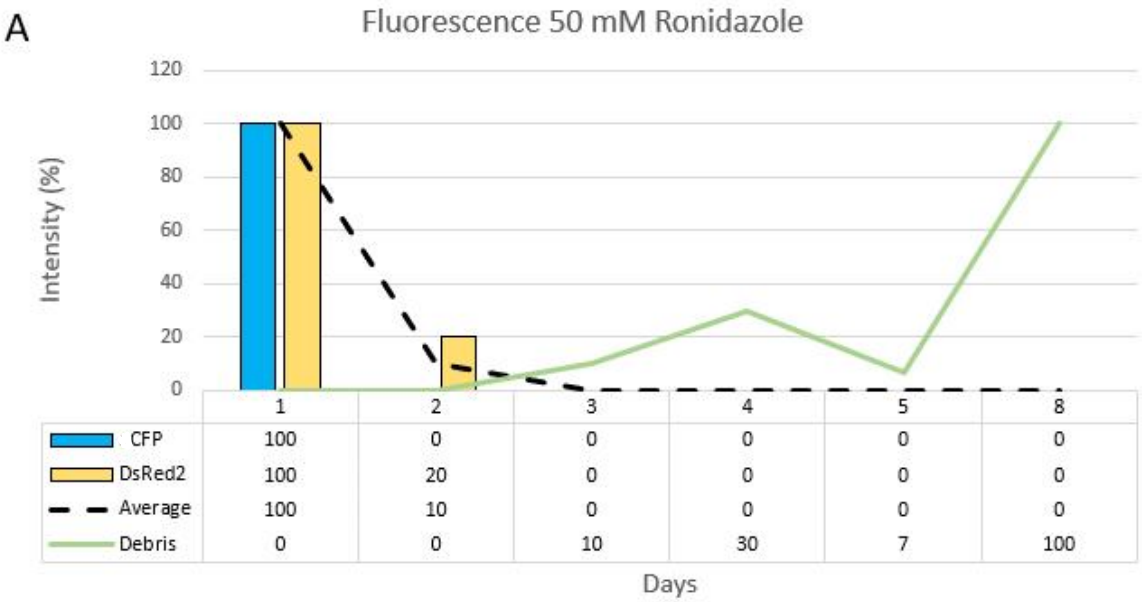

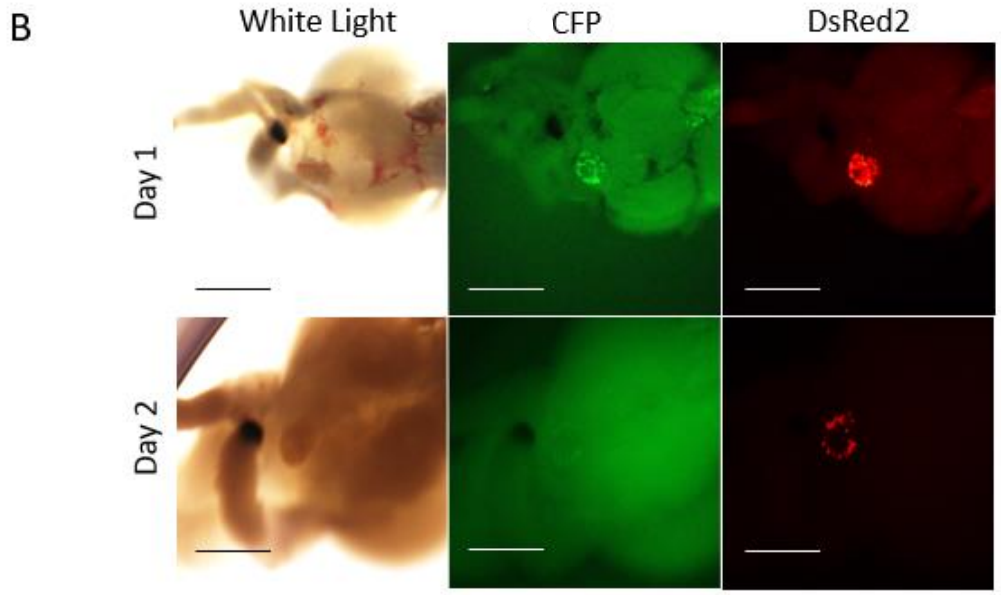

Figure 19: Fluorescence intensity monitoring of nfsB positive pituitary over 8 days in 50 mM ronidazole treatment. A) Fluorescence intensity of CFP (blue), DsRed2 (orange), average fluorescence (black) and amount of tissue debris (green) (n = 1). B) Imaged pituitary (oriented anterior to the left, posterior to the right) at days 1 and 2 in white light, CFP (green) and DsRed2 (red) (Magnification 2x; Scale bars = 1 mm).

When treating the tissue with 50 mM of RZ for 2 days, the fluorescence intensity effectively dropped to 0% in CFP and 20% in DsRed2 on day 2 (Figure 19). By day 3, the DsRed2 intensity dropped to 0%. The average fluorescence intensity thereby reached 0% by day 3 and remained low until the 8th day of the experiment. The amount of tissue debris remained low on day 1 to 5 but increased greatly on day 8 of the experiment.

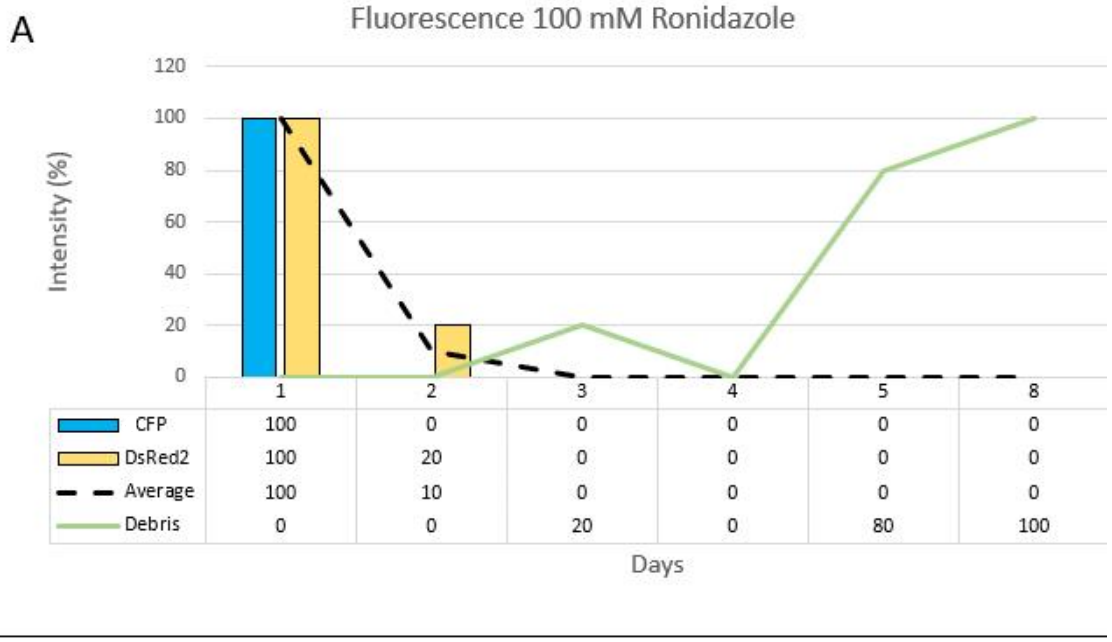

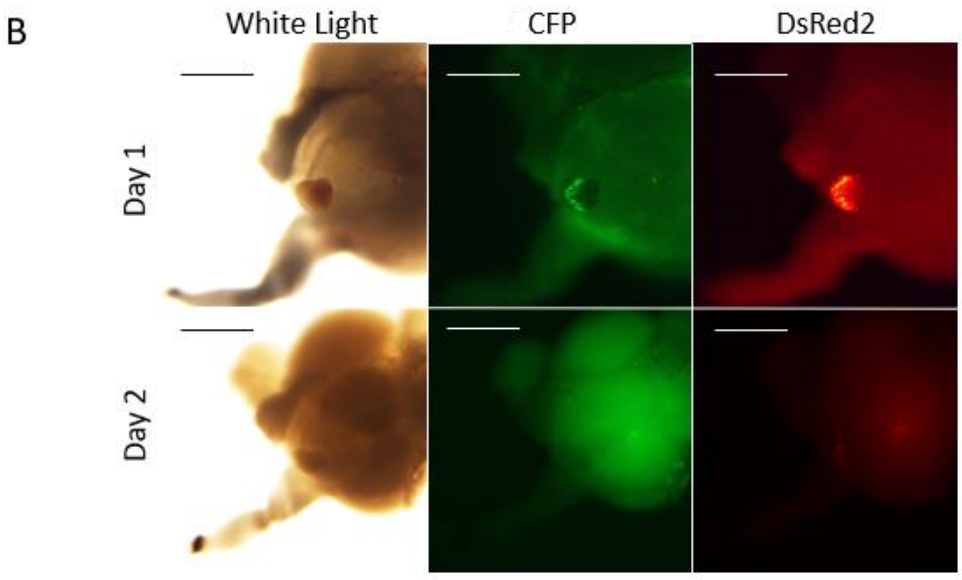

Figure 20: Fluorescence intensity monitoring of nfsB positive pituitary over 8 days in 100 mM ronidazole treatment. A) Fluorescence intensity of CFP (blue), DsRed2 (orange), average fluorescence (black) and amount of tissue debris (green) (n = 1). B) Imaged pituitary (oriented anterior to the left, posterior to the right) at days 1 and 2 in white light, CFP (green) and DsRed2 (red) (Magnification 2x; Scale bars = 1 mm).

When treating the tissue with 100 mM of RZ for 1 day, the fluorescence intensity effectively dropped to 0% in CFP and 20% in DsRed2 on day 2 (Figure 20). By day 3, the DsRed2 intensity also dropped to 0%. The average fluorescence intensity thereby reached 0% by day 3 and remained low until the 8th day of the experiment. Tissue debris increase remained low on day 1 to 4 but increased towards the last 2 days of the experiment.

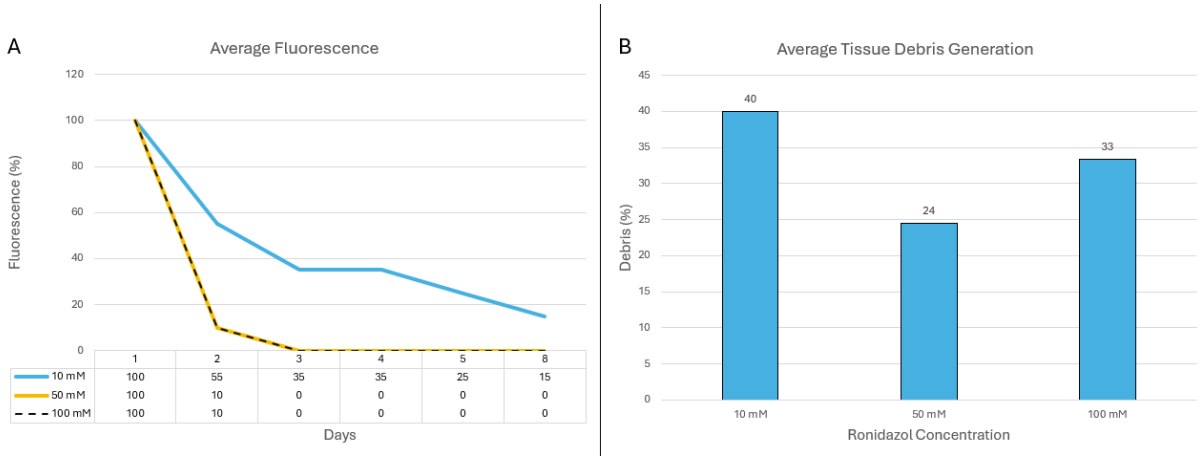

Figure 21: Comparison of the different concentrations of ronidazole based on daily average fluorescence intensity and weekly tissue debris amount. A) The average fluorescence intensity (both CFP and DsRed2) decreased slowly and did not reach 0% in the 10 mM Ronidazole treatment (blue). 50 mM (orange) and 100 mM (dotted black) treatments decreased the average fluorescence to 0% by day 3 (n = 1). B) The amount weekly tissue debris varied between the three concentrations 10 mM (40%), 50 mM (24%) and 100 mM (33%) (n = 1).

When comparing the daily average fluorescence of the three treatments, the 50 mM and 100 mM concentrations were most effective in reducing the fluorescence (Figure 21A). While 10 mM RZ treatment failed to completely decrease the fluorescence to 0% in 8 days of treatment, 50 mM and 100 mM seemed to induce 0% fluorescence by day 3. After stopping the RZ treatment the fluorescence intensity did not increase in any of the days for any of the tested concentrations, indicating no regrowth of Fsh cells. The weekly average tissue debris generation was also compared between the concentrations (Figure 21B). The 50 mM treatment seemed to show the lowest increase of tissue debris (24%), followed by 100 mM (33%) and 10 mM (40%).

Figure 22: Medaka brain on day 2 of the 100 mM Ronidazole treatment. Crystal formation emerged during the treatment but dissolved when Ronidazole was not supplied (Magnification = 1x).

Interestingly, the concentrations of 50 mM and 100 mM created crystal formations in the tissue cultures, which disappeared upon discontinuation of the treatment (Figure 22). To determine whether the different RZ concentrations and crystal formations impacted the health of the tissue, changes in cell nucleus morphology were investigated.

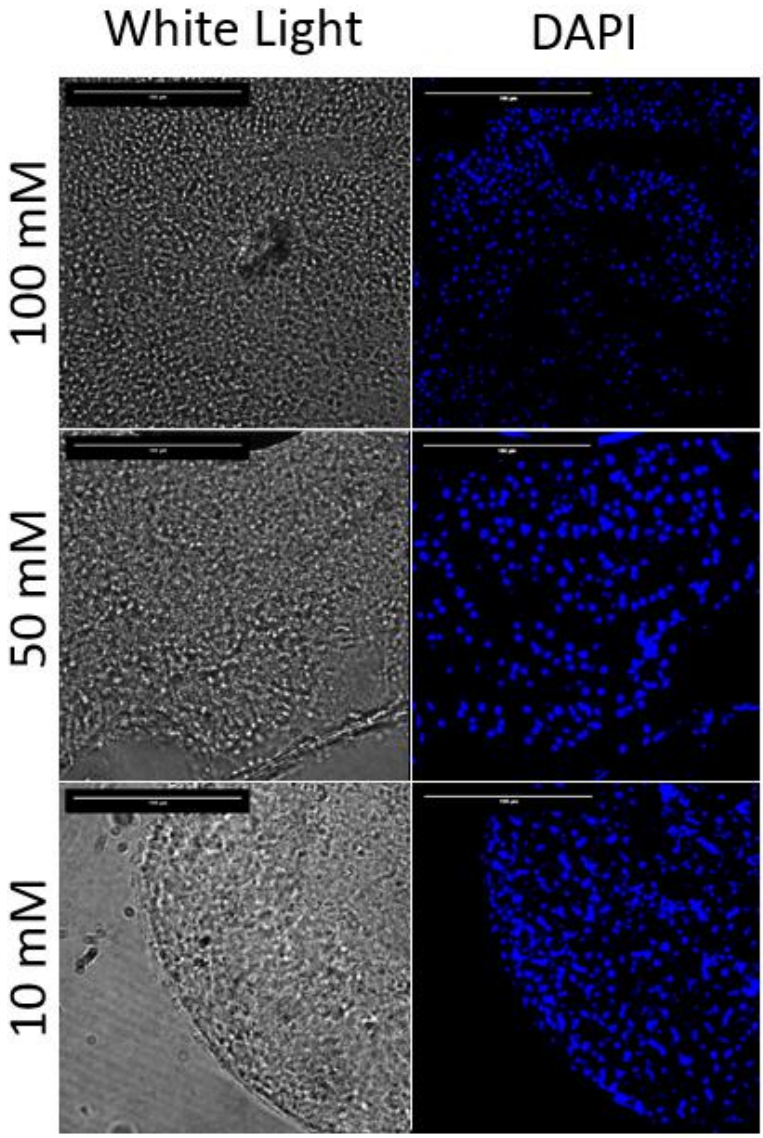

Figure 23: Brain- and pituitary tissue stained with DAPI. None of the concentrations indicated toxicity to the tissue (Magnification 63X; Scale bars = 100 μm).

Figure 23 shows that the cell nucleus morphology was round in all three concentrations, indicating no induction of apoptosis in cells not expressing NTR.

Ronidazole may therefore have led to specific cell ablation of Fsh cells, whereas cell recovery through fluorescence increase was not observed. The concentration of Ronidazole seemed to impact the effectiveness of NTR-driven ablation in whole-pituitary in this experiment. Unfortunately, due to time restrictions, the three concentrations were only tested once.

4. Discussion

This project aimed to generate two transgenic lines of medaka, tg(*tshbb*:tdTomato) and tg(*fshb*:NTR-CFP/*fshb:*DsRed2), for studying endocrine cells and their hormones in the pituitary. Furthermore, the aim was to use the tg(*fshb*:NTR-CFP/*fshb*:DsRed2) line to study tissue plasticity and regrowth following induced cell apoptosis of Fsh gonadotropes by the NTR/RZ system. The optimal tissue culture medium and CO_2 conditions were determined to successfully perform these experiments. The study successfully demonstrated transgenesis in fish, and how transgenic animals can be useful tools in NTR-mediated cell ablation of pituitary cells.

4.1 Generation of transgenic lines

4.1.1 Microinjection and egg development

To generate the transgenic lines, medaka eggs were injected with transgenic vectors supplied with the I-SceI Meganuclease to integrate the transgene plasmids *fshb*:NTR-CFP and *tshbb:*tdTomato into the genome. For microinjection of the plasmids, it was necessary to determine the optimal concentration of the transgenic DNA. Previous successful generations of transgenic fish lines suggested injecting 1 ng/µL (51), 10-30 ng/µL (72), and 50-100 ng/µL of the DNA vector (48), whereas 300 ng/µL could lead to survival rates as low as 3%. Concentration-related mortality has also been demonstrated in mice (73). While the increase from 10 to 40 ng/µL of injected DNA led to increased transgenesis success, the survival rate among the edited oocytes was also reduced. Microinjection volume may also affect mortality if exceeding 10% of the total cell volume (72). As the medaka egg volume is approximately 1 µL (61), this would require a maximum injection volume of 100 nL. The injected volume may be decreased by the high internal pressure of medaka eggs, where egg content (including injectant liquid) is pushed back into the needle (*personal observation*). This makes it hard to measure and control the exact injectant volume retained in the egg. To compensate for these parameters, the microinjection back-pressure is high, and the injection process begins- and ends outside of the medaka egg, as described in the Methods 2.4. This way, the total injection volume may be sufficient, while minimizing the morality rate.

4.1.1.1 tg(fshb:NTR-CFP/fshb:DsRed2)

To generate the tg(*fshb*:NTR-CFP/*fshb*:DsRed2) line in this project, eggs from the tg(*fshb:*DsRed2) line by Hodne et al were microinjected with the additional *fshb*:NTR-CFP plasmid (52).

In the generation of the tg(*fshb:*DsRed2) line, the article described that this transgenic line was created by injecting 10 µg/µL of the transgenic DNA vector. One protocol recommended this concentration (62), while being 1,000X higher than for many other developed transgenic lines. With this information in mind, it was suspected that the concentration unit in the article was misspelled and that they in fact injected 10 ng/µL. The mortality rate among injected eggs was unfortunately not described in this article. For this reason, positive tg(*fshb*:DsRed2) eggs were injected with a 10 ng/µL concentration of the *fshb*:NTR-CFP plasmid. This successfully generated the F0 founders of the tg(*fshb*:NTR-CFP/*fshb*:DsRed2) line in this project.

Positive hemizygous F0 fish were out-crossed to generate F1 offspring. When mature, 50% of these F1 fish screened positive for *nfsB*. This indicated a successful Mendelian distribution of the *fshb*:NTR:CFP plasmid, as depicted in Table 4. These positive fish were heterozygous (Tt) for the transgene. Intercrossed (Tt x Tt) F1 offspring created F2 eggs, where 65% tested positive for *nfsB*. When intercrossing heterozygous F1 fish, 75% of their offspring should be positive (50% heterozygous and 25% homozygous). With more screened individuals, the number of positive F2 individuals could be closer to 75%. As previously mentioned, F1 and F2 offspring were not screened for the *fshb*:DsRed2 transgene. For this reason, the positive fish could only be confirmed to carry the *fshb*:NTR:CFP plasmid. When comparing the fluorescence expression of the injected *fshb:*NTR-CFP to the pre-existing *fshb:*DsRed2 plasmid in the transgenic fish, there was a difference in fluorescence intensity. The 10 ng/µL injection led to weak CFP fluorescence compared to DsRed2. This could indicate overall weak expression of the entire *fshb:*NTR-CFP plasmid, which may impact the NTR effectiveness for future experiments.

4.1.1.2 tg(tshbb:tdTomato)

When developing the tg(*tshbb*:tdTomato) line, a high concentration of 250 ng/µL *tshbb*:tdTomato vector was used with the aim to improve the expression rate. This resulted in 24 fish that survived until adulthood after 3 months. 20 adult fish died before being screened for the transgene. Among the remaining fish, 1 F0 male tested positive to become the founder of the tg(*tshbb:*tdTomato) line. It was out-crossed with a WT female to create transgene positive F1 offspring. There was also an attempt to generate two additional transgenic lines of *tshba*:GFP and *sox2*:GFP with this DNA concentration, but only few survived 3 months post-injection. A second round of injection with 250 ng/µL resulted in 46 *tshbb*:tdTomato fish, 18 *tshba:*GFP fish, and 15 *sox2*:GFP fish that survived until adulthood. They all tested negative for their transgenes. The total survival rate among eggs was not measured.

Considering the DNA concentrations and volumes used for previous successful transgenic lines, it was suspected that the uncontrolled injection volume of 250 ng/µL of DNA too high. It was theorized that the eggs that grew up until adulthood, did so due to unsuccessful injection of the transgene, thus explaining the number of negative adult fish. By testing the concentrations 50-100 ng/µL, it could be interesting to see if the rate of survival and successful transgenesis increases.

All eggs were monitored to potentially detect fluorescence in Tshbb cells during development of F0 and F1 larvae. While the F0 eggs mostly showed auto-fluorescence and pigment fluorescence, the F1 generation descending from an out-crossed *nfsB*-positive F0 fish frequently showed an additional developing cell population between the eyes (Figure 12).

Considering that the F1 larvae were the offspring of a transgenic fish, it was suspected that this cell population could be *tshbb:*tdTomato expression. If this fluorescent population truly represents *tshbb*, the fact that these cells can be observed in the microscope can be groundbreaking. As previously described by Royan et al., *tshbb* expression is low or undetectable, especially in fish raised in long periods of light. In the Methods 2.2 about the rearing conditions, it was described that adult fish were kept in long light conditions (14h daylight; 10h night). This gave the same daylight cycle as the long light conditions tested in the article (14). For this reason, it was expected that a Tshbb cell population would not be observable in the microscope, at least not in adult fish. It is worth noting that the eggs were raised in dark incubators, with only short exposure to light for daily changes of the embryo culture medium. Previous studies have investigated the impact of photoperiod on melatonin

production, suggesting that constant darkness leads to high melatonin release in salmonids (74). As previously described, high melatonin levels increase *tshbb* expression in medaka. Since the tg(*tshbb*:tdTomato) F1 eggs were raised in dark conditions until hatching, it was suspected that these conditions could allow for higher *tshbb* expression in the egg stage, hence expressing the fluorescent tdTomato. While there are no studies describing the onset of either melatonin production or *tshbb* expression in developing medaka eggs, it would be interesting to compare the fluorescence of positive tg(*tshbb*:tdTomato) eggs in total darkness and continuous daylight to investigate this hypothesis. Further development of this transgenic line may allow for such investigations.

4.1.2 Screening issues and troubleshooting

A lot of the time consumption was due to problems with the PCR screening. Initially, a fast PCR kit (Phire Hot Start II DNA Polymerase, *Thermo Fischer*) was preferred for screening large numbers of individuals. While the fast Phire kit successfully screened the tg(*fshb*:NTR-CFP/*fshb*:DsRed2) line, the tg(*tshbb*:tdTomato) screening became challenging. Multiple primers were tested when screening for the *tdTomato* sequence, failing to amplify the transgene at any annealing temperatures (55-70 °C). New primers allowed the amplification of positive controls. This time a new problem emerged - all the samples screened positive, including the negative WT fish DNA control. The samples and controls even generated the correct primer band size described for *tdTomato*. For this reason, it was suspected cross-contamination in the DNA extraction process or master mix preparations. After screening the DNA extraction reagents, the water, and all PCR reagents, no contamination was found.

It was then suspected that the effectiveness of the fast Phire enzyme created high concentrations of amplified DNA, thus having a higher chance of contaminating neighboring wells in the electrophoresis gels. New WT samples were screened, absent of potential positive samples or positive controls in the sampling process and PCR. Additionally, the samples were separated with multiple empty wells to minimize the potential cross-contamination. This still resulted in bands in all the WT samples, with a band size indicating the presence of *tdTomato*. The BLAST tool by NCBI (*National Library of Medicine*; (75)) was used to search for the presence of the tdTomato sequence or any potential primer annealing points in the WT medaka genome, resulting in no matches. The forward- and reverse primers were also tested for potential dimer formation in the PCR process, but no dimers were found.

During the multiple failed PCR's and band extractions, most of the *tshbb:*tdTomato F0 fish had died of unknown reasons, leaving few animals to screen. A new combination of more specific primers depicted in Table 3 was tested. Here, one of the primers would anneal to the injected *tshbb* promoter sequence, while the other primer would anneal to the *tdTomato* sequence. These primers were unsuccessful in amplifying the transgene when tested in the fast Phire kit. This led to testing a slower PCR kit (Taq DNA Polymerase, *Thermo Scientific*) after successfully screening other transgenic lines. This time, a second band was revealed, making it possible to distinguish negative fish from positive *tshbb:*tdTomato fish.

The combination of primers and PCR protocol may explain this sudden successful screening for the *tshbb:*tdTomato plasmid. While the fast Phire kit successfully screened the tg(*fshb*:NTR-CFP/*fshb*:DsRed2) line, tg(*tshbb*:tdTomato) could only be screened with the slower Taq PCR protocol with these specific primers. Because of the time consumed in this troubleshooting, many fish were not screened for the respective transgenes.

4.2 Targeted ablation of ex vivo Fsh gonadotropes

The transgenic line tg(*fshb*:NTR-CFP/*fshb*:DsRed2) was used to demonstrate the practicality of transgenic lines in NTR-mediated ablation. Since NTR is co-expressed with fluorescent proteins, Fsh cell apoptosis induction could be observable under the fluorescence microscope. As previously mentioned, teleost fish have a remarkable ability for tissue regeneration. This project hypothesized that Fsh cells could potentially recover post-ablation.

4.2.1 Testing conditions

For performing specific ablation of Fsh cells in dissected tg(*fshb*:NTR-CFP/*fshb*:DsRed2) pituitary tissue, the tissue had to be kept alive in a tissue culture medium. Three different culture medias were tested for these experiments. Culture 1 (65) and Culture 2 (66) were both used for previous medaka cell- and tissue experiments. They were based on the L-15 medium (67), whereas the presence of Fetal Bovine Serum in Culture 1, and $NaHCO_3$ buffer in Culture 2 separated them. The two cultures were tested a couple of times (*data not shown*) before developing the third local Culture 3 by supplying $NaHCO_3$ to Culture 1. This resulted in a culture containing both Fetal Bovine Serum and $NaHCO_3$. The three cultures were then compared on the rate of tissue degradation over 8 days.

4.2.1.1 1% CO_2 Supplementation

Initially, the cultures were compared in a 1% CO_2 incubator. A multiple comparison test of the cultures revealed that the three cultures generated indifferent amounts of tissue debris when supplied with 1% CO_2. This led to using Culture 3 (with 1% CO_2) for some experiments. It was later learned that the main component of the cultures (L-15 medium) doesn't require CO_2 or $NaHCO_3$ supplementation.

CO_2 gas is commonly supplemented to cells and tissues in culture to maintain the pH within the physiological range. Since CO_2 dissolved in water creates carbonic acid, additional bicarbonate base ($NaHCO_3$) is supplied to allow pH buffering. However, Eagle H. (76) proved that added CO_2 (and $NaHCO_3$) was non-essential for keeping mouse fibroblasts healthy in culture, given daily medium change and substitutional buffer systems. The L-15 medium was later developed to eliminate the need for CO_2 and $NaHCO_3$ supplementation to ease the handling of cell cultures (67). The medium was instead buffered with phosphates and free base amino acids. This resulted in a culture medium able to buffer pH without the presence of CO_2 and $NaHCO_3$, given the daily replacement of the culture medium.

In this project, the pH of Culture 1 was only buffered by the L-15 medium components, whereas Culture 2 and 3 additionally contained $NaHCO_3$ buffer. The fact that the tissue in Culture 1 wasn't significantly affected by CO_2 acidity, proves the compensating buffer capacity of the L-15 medium. The L-15 medium contains the phenol red indicator, which allowed observation of pH changes in the cultures. As suspected, the color of Culture 1 indicated a slight decrease in pH after 24 hours, while the pH of Culture 2 and 3 mostly remained stable (*data not shown).* The fact that Culture 2 and 3 contained more buffer than Culture 1, could have impacted the pH.

4.2.1.2 0% CO_2 Supplementation

The three cultures were then compared in an incubator with 0% CO_2 supplementation. When keeping the cultures in 0% CO_2 (as the L-15 medium was developed for), Culture 1 generated significantly less tissue degradation than the other cultures at the last day of the experiment, with generally low amounts of debris throughout the week. By observing the medium pH indicator, the pH only slightly decreased most of the experiment days (*data not shown*). Regarding the different compositions of the culture mediums, Culture 1 is the only medium

following the composition recommendations of the original paper for the L-15 culture development, meaning that it contains Fetal Bovine Serum and lacks $NaHCO_3$ in 0% CO_2.

In comparison, Culture 2 generated significantly higher amounts of tissue degradation than the other culture mediums already on day 3. The pH had slightly increased in Cultures 2 and 3, which could be explained by excess alkaline ($NaHCO_3$) in the medium. It was for this reason suspected that this created culture conditions too alkaline for keeping medaka pituitary tissue healthy. Through comparisons, CO_2 concentration didn't seem to significantly impact overall daily tissue degradation or the specific culture medium variants. Since two different culture medium variants were used in different CO2 concentrations for the ronidazole experiments, it was interesting to see if there was a significant difference between these conditions. On the 8^{th} day of treatment, Culture 3 (1% CO_2) generated a significantly higher degree of tissue degradation than Culture 1 (0% CO_2).

This could concludingly suggest that the latter condition should be recommended for ex vivo experiments. Considering these results, it could have been interesting to test if Culture 1 (0% CO_2) could maintain the medaka brain- and pituitary tissue for experiments even longer than 8 days.

It is worth noting that contamination occurred in many tissue samples in culture medium during these experiments. To avoid this, the well plates were never opened outside of the sterile bench, and imaging of tissue was performed with the lid on (which impacted image quality). An alternative is to transfer tissue for imaging to a Petri dish containing dPBS in the sterile bench. The forceps or spatula used to transfer the tissue was disinfected between the handling of different tissue samples. This dish can be moved to a microscope while minimizing contamination of the culture medium and improving image quality.

4.2.2 NTR-driven ablation

First, the successful integration of the transgenes in the Fsh cells had to be verified in positive *nfsB* fish from the tg(*fshb*:NTR-CFP/*fshb*:DsRed2) line. By slicing the pituitary tissue of a positively screened F1 fish, it could be confirmed that CFP and DsRed2 were expressed in the same cells. This indicated that these cells expressed both microinjected plasmids (*fshb*:DsRed2 and *fshb*:NTR:CFP), and that NTR-driven ablation of Fsh cells could be observed in the microscope. Due to the limitations of time, animals, and thus the number of

experiments, it is important to keep in mind that the following observations in this project were not supported by statistics. Therefore, the interpretations of these results only illustrate what tendencies of NTR-mediated Fsh cell ablation may look like. Further experiments are therefore needed to potentially confirm these preliminary results.

Previous experiments of NTR-mediated cell ablation in zebrafish had successfully treated whole larvae with metronidazole concentrations of 0.1 mM to 10 mM (77). It was shown that effective neutrophil ablation was performed at concentrations as low as 0.1 mM, while higher concentrations increased larvae mortality rates. Since neutrophils usually exist as single cells in the blood, it was suspected that higher doses were needed for cells in whole pituitary tissue. Another study performed successful cell ablation using 5 mM and 10 mM MTZ (for 1 – 3 days) in whole zebrafish brain- and pituitary tissue (78). Previous studies also compared the tolerance and efficiency of MTZ to its derivative ronidazole in whole zebrafish larvae (79). The study demonstrated that a 3-day treatment showed a tolerance of up to 15 mM MTZ and 8 mM RZ. RZ was also shown to have a 10X higher cell ablation efficiency, meaning treatments could be done at lower concentrations.

4.2.2.1 10 mM Ronidazole

RZ was therefore used for the potential ablation of Fsh cells in the whole pituitary tissue of medaka in this project. A high concentration of 10 mM RZ was initially tested, with plans of titrating the treatment concentrations to an ideal number. Despite co-expression of the injected transgenes, while CFP fluorescence decreased after 1 day of treatment, DsRed2 remained visible even after 8 days of treatment. The difference in fluorescence reduction was suspected to be linked to differences in brightness and half-life of CFP and DsRed2. While DsRed2 fluorescence is twice as bright as CFP (80,81), no papers were found to compare the half-lives of these proteins in vivo. Another hypothesis was that the injected concentration of 10 ng/µL *fshb*:NTR:CFP plasmid gave weak fluorescence of CFP, as previously described. If this plasmid concentration resulted in low CFP expression, the NTR expression may also have been reduced, thus reducing the chance of successful Fsh cell ablation. The fact that DsRed2 (which indicates *fshb* expression) still is visible after 8 days of treatment illustrates that apoptosis induction with 10 mM RZ was ineffective in the Fsh cells. Furthermore, it was decided to increase the RZ concentrations to 50 mM and 100 mM to increase ablation efficiency.

4.2.2.2 High Concentration Treatment

In contrary to 10 mM treatments, the high concentrations (50 mM and 100 mM) seemed more effective in fluorescence reduction, indicating successful Fsh ablation. Interestingly, crystal formations developed in the culture mediums of high RZ concentrations. These crystals dissolved upon discontinuation of RZ supplementation. While the efficient reduction in fluorescence was demonstrated, it was unknown if this was due to Fsh-specific cell ablation or general toxicity from the high RZ concentrations. It is worth noting that 50 mM and 100 mM RZ theoretically correspond to the efficiency of 500mM and 1000 mM MTZ, respectively. These are concentrations never tested in any species, as max RZ tolerance has been reported at 15 mM in whole zebrafish larvae.

Through comparison of tissue debris generation, it seemed like 10 mM RZ generated more tissue debris, than in high concentration treatments. This could be linked to the previous discoveries about the culture conditions. Additionally, the DAPI stains of the pituitary nuclei revealed perfectly round nuclei in all concentrations, suggesting that the tissue seemed healthy at RZ concentrations as high as 100 mM. Additionally, the aim of this project was to potentially observe regeneration of ablated Fsh cells. Even though the high concentration treatments were performed in the best suggested culture conditions, the recovery of Fsh cells was not observed after stopping the RZ treatment. Considering these observations, it could be hypothesized that reduction in the fluorescent markers could be caused by targeted Fsh cell ablation and not by toxicity. If so, the Fsh cells may need more time (than 6-7 days) to potentially recover. To confirm this, additional tests must be carried out.

4.2.2.3 Ablation efficiency

Though there was observed an efficiency difference between the RZ concentrations, it is worth noting that the natural fluorescence reduction in *nfsB*-positive Fsh cells without RZ treatment was unknown. The tg(*fshb*:NTR-CFP/*fshb*:DsRed2) line was not screened for the *fshb*:DsRed2 control transgene, resulting in many *nfsB*-positive fish not expressing DsRed2. The NTR-driven ablation of Fsh cells could not be confirmed without the expression of this transgene. Therefore, tissue co-expressing both transgenes was saved for the RZ treatments. Several brain- and pituitary tissues only expressing the *fshb*:NTR-CFP plasmid was used as negative controls (no RZ treatment) to potentially observe this natural fluorescence reduction, but most suffered from contamination early in the experiments.

Although high RZ concentrations were required for Fsh ablation in this transgenic line, no articles requiring 50 or 100 mM RZ for NTR-mediated ablation were found. The requirement of concentrations this high, may be correlated with the low injection concentration in addition to the variant of the NTR gene. In this tg(*fshb*:NTR-CFP/*fshb*:DsRed2) line, the *nfsB* sequence in is derived from wildtype E. coli (NCBI ID: WP_000351487.1). Some studies have described that native NTR variants require relatively high concentrations of MTZ, as observed in this project. Several NTR mutants were therefore developed to increase NTR sensitivity to MTZ, thus improving ablation efficiency. These mutants required lower MTZ concentrations for successful ablation (82,83).

Assuming this efficiency was negatively affected by low concentration of a less effective NTR gene, a new tg(*fshb*:NTR-CFP/*fshb*:DsRed2) line could be developed. To potentially develop this line, 50-100 ng/µL of the new transgenic plasmid should be injected. Here, the NTR sequence should be replaced with a more efficient NTR mutant. To confirm the complete ablation of cells expressing *fshb*, the presence of both *fshb:*NTR-CFP and *fshb*:DsRed2 transgenes must be confirmed with PCR. This will identify more fish co-expressing the *fshb*-inducating DsRed2. Another variable to consider is that the majority of the transgenic F1 and F2 were heterozygous (Tt), meaning that the transgene only is carried in 1 of 2 chromosome pairs. By further developing this transgenic line, homozygous (TT) individuals might be identified. These fish might show even more intense fluorescence of the transgenes, which could improve the performance of ex vivo experiments. By performing the treatments in Culture 1 (0% CO_2), the experiments may also last longer than 8 days. This way the remarkable regenerative ability of the Japanese medaka may be demonstrated in Fsh gonadotropes.

5. Conclusion

This study shows that transgenic lines of medaka can be developed and utilized as tools for studying the pituitary cells. The basis of two transgenic lines were established for studying Tshbb and Fsh cells in the teleost model fish medaka. Tg(*tshbb:*tdTomato) larvae produced a fluorescent cell population between the eyes, which could depict the first visualization of the Tshbb expressing cells. By further developing this line, these pituitary cells may be studied for the first time in vivo in medaka.

Tg(*fshb*:NTR-CFP/*fshb*:DsRed2) pituitary tissue was used in ex vivo treatment with ronidazole to induce Fsh cell specific apoptosis. Among the tested culture conditions for these treatments, the culture medium by Karigo et al. (65) with no CO_2 supplementation performed best in retaining tissue health. For successfully inducing effective Fsh cell ablation with ronidazole, extremely high concentrations (50 mM to 100 mM) were required in this transgenic line. The cell regeneration could not be observed. By further developing this line, homozygous fish with stronger transgenic expression may be helpful for further ablation experiments. This can reduce the required concentrations needed for targeted cell ablation. By performing the ex vivo experiments in good culture conditions, the duration may be extended and Fsh cell regeneration can hopefully be observed under the microscope.

Though many issues emerged during this project, two transgenic lines were founded. By continuing to develop these lines, they can be useful tools for studying the remarkable endocrine system and regenerative abilities of the medaka. These tools and findings can together create the basis for in-depth investigation of how gonadotrope and thyrotrope cells can adapt to meet hormone demands.

6. References

1. Santiago-Andres Y, Golan M, Fiordelisio T. Functional Pituitary Networks in Vertebrates. Front Endocrinol (Lausanne) 2021;11:619352. https://doi.org/10.3389/fendo.2020.619352.
2. Weltzien F-A, Hildahl J, Hodne K, Okubo K, Haug TM. Embryonic development of gonadotrope cells and gonadotropic hormones – Lessons from model fish. Molecular and Cellular Endocrinology 2014;385:18–27. https://doi.org/10.1016/j.mce.2013.10.016.
3. Fontaine R, Rahmad Royan M, Henkel C, Hodne K, Ager-Wick E, Weltzien F-A. Pituitary multi-hormone cells in mammals and fish: history, origin, and roles. Frontiers in Neuroendocrinology 2022;67:101018. https://doi.org/10.1016/j.yfrne.2022.101018.
4. Gleiberman AS, Michurina T, Encinas JM, Roig JL, Krasnov P, Balordi F, et al. Genetic approaches identify adult pituitary stem cells. Proceedings of the National Academy of Sciences 2008;105:6332–7. https://doi.org/10.1073/pnas.0801644105.
5. Royan MR, Siddique K, Csucs G, Puchades MA, Nourizadeh-Lillabadi R, Bjaalie JG, et al. 3D Atlas of the Pituitary Gland of the Model Fish Medaka (Oryzias latipes). Frontiers in Endocrinology 2021;12.
6. Pirahanchi Y, Toro F, Jialal I. Physiology, Thyroid Stimulating Hormone. StatPearls, Treasure Island (FL): StatPearls Publishing; 2023.
7. Gonadotropins. LiverTox: Clinical and Research Information on Drug-Induced Liver Injury, Bethesda (MD): National Institute of Diabetes and Digestive and Kidney Diseases; 2012.
8. Levavi-Sivan B, Bogerd J, Mañanós EL, Gómez A, Lareyre JJ. Perspectives on fish gonadotropins and their receptors. General and Comparative Endocrinology 2010;165:412–37. https://doi.org/10.1016/j.ygcen.2009.07.019.
9. Hsu SY, Nakabayashi K, Bhalla A. Evolution of Glycoprotein Hormone Subunit Genes in Bilateral Metazoa: Identification of Two Novel Human Glycoprotein Hormone Subunit Family Genes, GPA2 and GPB5. Molecular Endocrinology 2002;16:1538–51. https://doi.org/10.1210/mend.16.7.0871.
10. Hiller-Sturmhöfel S, Bartke A. The Endocrine System. Alcohol Health Res World 1998;22:153–64.
11. Brown ME. The Physiology of Fishes: Metabolism. Academic Press; 2013.
12. Maugars G, Dufour S, Cohen-Tannoudji J, Quérat B. Multiple thyrotropin β-subunit and thyrotropin receptor-related genes arose during vertebrate evolution. PLoS One 2014;9:e111361. https://doi.org/10.1371/journal.pone.0111361.
13. Fleming MS, Maugars G, Lafont A-G, Rancon J, Fontaine R, Nourizadeh-Lillabadi R, et al. Functional divergence of thyrotropin beta-subunit paralogs gives new insights into salmon smoltification metamorphosis. Sci Rep 2019;9:4561. https://doi.org/10.1038/s41598-019-40019-5.
14. Royan MR, Hodne K, Nourizadeh-Lillabadi R, Weltzien F-A, Henkel C, Fontaine R. Day length regulates gonadotrope proliferation and reproduction via an intra-pituitary pathway in the model vertebrate Oryzias latipes. Commun Biol 2024;7:1–13. https://doi.org/10.1038/s42003-024-06059-y.
15. Irachi S, Hall DJ, Fleming MS, Maugars G, Björnsson BT, Dufour S, et al. Photoperiodic regulation of pituitary thyroid-stimulating hormone and brain deiodinase in Atlantic salmon. Molecular and Cellular Endocrinology 2021;519:111056. https://doi.org/10.1016/j.mce.2020.111056.

16. Nedresky D, Singh G. Physiology, Luteinizing Hormone. StatPearls, Treasure Island (FL): StatPearls Publishing; 2024.
17. Barbieri RL. The Endocrinology of the Menstrual Cycle. In: Rosenwaks Z, Wassarman PM, editors. Human Fertility, vol. 1154, New York, NY: Springer New York; 2014, p. 145–69. https://doi.org/10.1007/978-1-4939-0659-8_7.
18. Orlowski M, Sarao MS. Physiology, Follicle Stimulating Hormone. StatPearls, Treasure Island (FL): StatPearls Publishing; 2024.
19. Zohar Y, Muñoz-Cueto JA, Elizur A, Kah O. Neuroendocrinology of reproduction in teleost fish. General and Comparative Endocrinology 2010;165:438–55. https://doi.org/10.1016/j.ygcen.2009.04.017.
20. Le Tissier PR, Murray JF, Mollard P. A New Perspective on Regulation of Pituitary Plasticity: The Network of SOX2-Positive Cells May Coordinate Responses to Challenge. Endocrinology 2022;163:bqac089. https://doi.org/10.1210/endocr/bqac089.
21. Le Tissier PR, Hodson DJ, Lafont C, Fontanaud P, Schaeffer M, Mollard P. Anterior pituitary cell networks. Frontiers in Neuroendocrinology 2012;33:252–66. https://doi.org/10.1016/j.yfrne.2012.08.002.
22. Totipotent Stem Cell - an overview | ScienceDirect Topics n.d. https://www.sciencedirect.com/topics/medicine-and-dentistry/totipotent-stem-cell (accessed March 14, 2024).
23. Jopling C, Boue S, Belmonte JCI. Dedifferentiation, transdifferentiation and reprogramming: three routes to regeneration. Nat Rev Mol Cell Biol 2011;12:79–89. https://doi.org/10.1038/nrm3043.
24. Fontaine R, Ager-Wick E, Hodne K, Weltzien F-A. Plasticity of Lh cells caused by cell proliferation and recruitment of existing cells. J Endocrinol 2019;240:361–77. https://doi.org/10.1530/JOE-18-0412.
25. Yamanaka S, Blau HM. Nuclear reprogramming to a pluripotent state by three approaches. Nature 2010;465:704–12. https://doi.org/10.1038/nature09229.
26. Jopling C, Sleep E, Raya M, Martí M, Raya A, Belmonte JCI. Zebrafish heart regeneration occurs by cardiomyocyte dedifferentiation and proliferation. Nature 2010;464:606–9. https://doi.org/10.1038/nature08899.
27. Guo M, Hay BA. Cell proliferation and apoptosis. Current Opinion in Cell Biology 1999;11:745–52. https://doi.org/10.1016/S0955-0674(99)00046-0.
28. Phylum Chordata. Fishes of the World, John Wiley & Sons, Ltd; 2016, p. 13–526. https://doi.org/10.1002/9781119174844.ch2.
29. PARENTI LR. A phylogenetic analysis and taxonomic revision of ricefishes, Oryzias and relatives (Beloniformes, Adrianichthyidae). Zoological Journal of the Linnean Society 2008;154:494–610. https://doi.org/10.1111/j.1096-3642.2008.00417.x.
30. Assorted Medaka Ricefish aka Japanese Ricefish/Killifish (Oryzias latipes) - Tank-Bred! Aquatic Arts n.d. https://aquaticarts.com/products/assorted-medaka-ricefish (accessed May 9, 2024).
31. Naruse K, Tanaka M, Takeda H, editors. Medaka. Tokyo: Springer Japan; 2011. https://doi.org/10.1007/978-4-431-92691-7.
32. Katogi R, Nakatani Y, Shin-i T, Kohara Y, Inohaya K, Kudo A. Large-scale analysis of the genes involved in fin regeneration and blastema formation in the medaka, Oryzias latipes. Mechanisms of Development 2004;121:861–72. https://doi.org/10.1016/j.mod.2004.03.015.

33. Shima A, Mitani H. Medaka as a research organism: past, present and future. Mechanisms of Development 2004;121:599–604. https://doi.org/10.1016/j.mod.2004.03.011.
34. Oryzias latipes. NCBI n.d. https://www.ncbi.nlm.nih.gov/datasets/taxonomy/8090/ (accessed February 26, 2024).
35. Danio rerio genome assembly GRCz11. NCBI n.d. https://www.ncbi.nlm.nih.gov/data-hub/assembly/GCF_000002035.6/ (accessed April 11, 2024).
36. Oryzias latipes genome assembly ASM223467v1. NCBI n.d. https://www.ncbi.nlm.nih.gov/data-hub/assembly/GCF_002234675.1/ (accessed April 11, 2024).
37. Ulloa PE, Iturra P, Neira R, Araneda C. Zebrafish as a model organism for nutrition and growth: towards comparative studies of nutritional genomics applied to aquacultured fishes. Rev Fish Biol Fisheries 2011;21:649–66. https://doi.org/10.1007/s11160-011-9203-0.
38. Fontaine R, Ager-Wick E, Hodne K, Weltzien F-A. Plasticity in medaka gonadotropes via cell proliferation and phenotypic conversion. J Endocrinol 2020;245:21–37. https://doi.org/10.1530/JOE-19-0405.
39. Royan MR, Kayo D, Weltzien F-A, Fontaine R. Sexually Dimorphic Regulation of Gonadotrope Cell Hyperplasia in Medaka Pituitary via Mitosis and Transdifferentiation. Endocrinology 2023;164:bqad030. https://doi.org/10.1210/endocr/bqad030.
40. Alunni A, Hermel J-M, Heuzé A, Bourrat F, Jamen F, Joly J-S. Evidence for neural stem cells in the medaka optic tectum proliferation zones. Developmental Neurobiology 2010;70:693–713. https://doi.org/10.1002/dneu.20799.
41. Royan MR, Hodne K, Nourizadeh-lillabadi R, Weltzien F-A, Henkel CV, Fontaine R. Photoperiod regulates gonadotrope cell division in medaka via melatonin, Tsh and folliculostellate cells 2023:2023.06.09.544159. https://doi.org/10.1101/2023.06.09.544159.
42. Gordon JW, Ruddle FH. Integration and Stable Germ Line Transmission of Genes Injected into Mouse Pronuclei. Science 1981;214:1244–6. https://doi.org/10.1126/science.6272397.
43. Ahmad A, Jamil A, Munawar N. GMOs or non-GMOs? The CRISPR Conundrum. Front Plant Sci 2023;14:1232938. https://doi.org/10.3389/fpls.2023.1232938.
44. Rubin GM, Spradling AC. Genetic transformation of Drosophila with transposable element vectors. Science 1982;218:348–53. https://doi.org/10.1126/science.6289436.
45. Gordon JW, Ruddle FH. DNA-mediated genetic transformation of mouse embryos and bone marrow--a review. Gene 1985;33:121–36. https://doi.org/10.1016/0378-1119(85)90087-3.
46. McMahon AP, Novak TJ, Britten RJ, Davidson EH. Inducible expression of a cloned heat shock fusion gene in sea urchin embryos. Proceedings of the National Academy of Sciences 1984;81:7490–4. https://doi.org/10.1073/pnas.81.23.7490.
47. Etkin LD. Analysis of the Mechanisms Involved in Gene Regulation and Cell Differentiation by Microinjection of Purified Genes and Somatic Cell Nuclei into Amphibian Oocytes and Eggs. Differentiation 1982;21:149–59. https://doi.org/10.1111/j.1432-0436.1982.tb01208.x.
48. Stuart GW, Mcmurray JV, Westerfield M. Replication, integration and stable germ-line transmission of foreign sequences injected into early zebrafish embryos. Development 1988;103:403–12. https://doi.org/10.1242/dev.103.2.403.

49. Tröder SE, Zevnik B. History of genome editing: From meganucleases to CRISPR. Lab Anim 2022;56:60–8. https://doi.org/10.1177/0023677221994613.
50. Thermes V, Grabher C, Ristoratore F, Bourrat F, Choulika A, Wittbrodt J, et al. I-SceI meganuclease mediates highly efficient transgenesis in fish. Mechanisms of Development 2002;118:91–8. https://doi.org/10.1016/S0925-4773(02)00218-6.
51. Hildahl J, Sandvik GK, Lifjeld R, Hodne K, Nagahama Y, Haug TM, et al. Developmental tracing of luteinizing hormone β-subunit gene expression using green fluorescent protein transgenic medaka (Oryzias latipes) reveals a putative novel developmental function. Developmental Dynamics 2012;241:1665–77. https://doi.org/10.1002/dvdy.23860.
52. Hodne K, Fontaine R, Ager-Wick E, Weltzien F-A. Gnrh1-Induced Responses Are Indirect in Female Medaka Fsh Cells, Generated Through Cellular Networks. Endocrinology 2019;160:3018–32. https://doi.org/10.1210/en.2019-00595.
53. Takahashi A, Islam MS, Abe H, Okubo K, Akazome Y, Kaneko T, et al. Morphological analysis of the early development of telencephalic and diencephalic gonadotropin-releasing hormone neuronal systems in enhanced green fluorescent protein-expressing transgenic medaka lines. J Comp Neurol 2016;524:896–913. https://doi.org/10.1002/cne.23883.
54. Clark A, Iwobi M, Cui W, Crompton M, Harold G, Hobbs S, et al. Selective cell ablation in transgenic mice expressing E. coli nitroreductase. Gene Ther 1997;4:101–10. https://doi.org/10.1038/sj.gt.3300367.
55. Willems B, Büttner A, Huysseune A, Renn J, Witten PE, Winkler C. Conditional ablation of osteoblasts in medaka. Developmental Biology 2012;364:128–37. https://doi.org/10.1016/j.ydbio.2012.01.023.
56. Tabor KM, Bergeron SA, Horstick EJ, Jordan DC, Aho V, Porkka-Heiskanen T, et al. Direct activation of the Mauthner cell by electric field pulses drives ultrarapid escape responses. J Neurophysiol 2014;112:834–44. https://doi.org/10.1152/jn.00228.2014.
57. Otsuka T, Takeda H. Targeted Ablation of Pancreatic β Cells in Medaka. Jzoo 2017;34:179–84. https://doi.org/10.2108/zs170004.
58. Transgenic n.d. https://www.genome.gov/genetics-glossary/Transgenic (accessed January 10, 2024).
59. Curado S, Anderson RM, Jungblut B, Mumm J, Schroeter E, Stainier DYR. Conditional targeted cell ablation in zebrafish: A new tool for regeneration studies. Developmental Dynamics 2007;236:1025–35. https://doi.org/10.1002/dvdy.21100.
60. Kinoshita M, Murata K, Naruse K, Tanaka M. Medaka: Biology, Management, and Experimental Protocols. John Wiley & Sons; 2009.
61. Iwamatsu T. Stages of normal development in the medaka Oryzias latipes. Mechanisms of Development 2004;121:605–18. https://doi.org/10.1016/j.mod.2004.03.012.
62. Thumberger T, Stobrawa S, Wittbrodt J. Microinjection in early embryos of Zebrafish and Medaka: From Transgenesis to CRISPR n.d.
63. Gupta RS, Chan DYH, Siminovitch L. Evidence for functional hemizygosity at the Emtr locus in CHO cells through segregation analysis. Cell 1978;14:1007–13. https://doi.org/10.1016/0092-8674(78)90354-9.
64. Fontaine R, Hodne K, Weltzien F-A. Healthy Brain-pituitary Slices for Electrophysiological Investigations of Pituitary Cells in Teleost Fish. J Vis Exp 2018:57790. https://doi.org/10.3791/57790.

65. Karigo T, Kanda S, Takahashi A, Abe H, Okubo K, Oka Y. Time-of-Day-Dependent Changes in GnRH1 Neuronal Activities and Gonadotropin mRNA Expression in a Daily Spawning Fish, Medaka. Endocrinology 2012;153:3394–404. https://doi.org/10.1210/en.2011-2022.
66. Ager-Wick E, Hodne K, Fontaine R, von Krogh K, Haug TM, Weltzien F-A. Preparation of a High-quality Primary Cell Culture from Fish Pituitaries. J Vis Exp 2018:58159. https://doi.org/10.3791/58159.
67. LEIBOVITZ A. THE GROWTH AND MAINTENANCE OF TISSUE–CELL CULTURES IN FREE GAS EXCHANGE WITH THE ATMOSPHERE1. American Journal of Epidemiology 1963;78:173–80. https://doi.org/10.1093/oxfordjournals.aje.a120336.
68. Elmore S. Apoptosis: A Review of Programmed Cell Death. Toxicol Pathol 2007;35:495–516. https://doi.org/10.1080/01926230701320337.
69. Excitation and emission information for Living Colors fluorescent proteins n.d. https://www.takarabio.com/learning-centers/gene-function/fluorescent-proteins/fluorescent-protein-excitation-and-emission-maxima (accessed April 8, 2024).
70. Licea-Rodriguez J, Figueroa-Melendez A, Falaggis K, Sánchez MP, Riquelme M, Rocha-Mendoza I. Multicolor fluorescence microscopy using static light sheets and a single-channel detection. JBO 2019;24:016501. https://doi.org/10.1117/1.JBO.24.1.016501.
71. Schindelin J, Arganda-Carreras I, Frise E, Kaynig V, Longair M, Pietzsch T, et al. Fiji: an open-source platform for biological-image analysis. Nat Methods 2012;9:676–82. https://doi.org/10.1038/nmeth.2019.
72. Grabher C, Wittbrodt J. Recent Advances in Meganuclease-and Transposon-Mediated Transgenesis of Medaka and Zebrafish. In: Sharpe PT, Mason I, editors. Molecular Embryology: Methods and Protocols, Totowa, NJ: Humana Press; 2009, p. 521–39. https://doi.org/10.1007/978-1-60327-483-8_36.
73. Factors affecting the efficiency of introducing foreign DNA into mice by microinjecting eggs. n.d. https://doi.org/10.1073/pnas.82.13.4438.
74. Iigo M, Abe T, Kambayashi S, Oikawa K, Masuda T, Mizusawa K, et al. Lack of circadian regulation of *in vitro* melatonin release from the pineal organ of salmonid teleosts. General and Comparative Endocrinology 2007;154:91–7. https://doi.org/10.1016/j.ygcen.2007.06.013.
75. BLAST: Basic Local Alignment Search Tool n.d. https://blast.ncbi.nlm.nih.gov/Blast.cgi (accessed November 24, 2022).
76. Eagle H. The salt requirements of mammalian cells in tissue culture. Archives of Biochemistry and Biophysics 1956;61:356–66. https://doi.org/10.1016/0003-9861(56)90358-7.
77. Hall CJ, Astin JW, Mumm JS, Ackerley DF. A New Transgenic Line for Rapid and Complete Neutrophil Ablation. Zebrafish 2022;19:109–13. https://doi.org/10.1089/zeb.2022.0020.
78. Gutnick A, Blechman J, Kaslin J, Herwig L, Belting H-G, Affolter M, et al. The Hypothalamic Neuropeptide Oxytocin Is Required for Formation of the Neurovascular Interface of the Pituitary. Dev Cell 2011;21:642–54. https://doi.org/10.1016/j.devcel.2011.09.004.
79. Lai S, Kumari A, Liu J, Zhang Y, Zhang W, Yen K, et al. Chemical screening reveals Ronidazole is a superior prodrug to Metronidazole for nitroreductase-induced cell ablation system in zebrafish larvae. Journal of Genetics and Genomics 2021;48:1081–90. https://doi.org/10.1016/j.jgg.2021.07.015.
80. Lambert T. DsRed2 at FPbase. FPbase n.d. https://www.fpbase.org/protein/dsred2/ (accessed May 6, 2024).
81. Lambert T. ECFP at FPbase. FPbase n.d. https://www.fpbase.org/protein/ecfp/ (accessed May 6, 2024).

82. Sharrock AV, Mulligan TS, Hall KR, Williams EM, White DT, Zhang L, et al. NTR 2.0: a rationally engineered prodrug-converting enzyme with substantially enhanced efficacy for targeted cell ablation. Nat Methods 2022;19:205–15. https://doi.org/10.1038/s41592-021-01364-4.
83. Mathias JR, Zhang Z, Saxena MT, Mumm JS. Enhanced Cell-Specific Ablation in Zebrafish Using a Triple Mutant of Escherichia Coli Nitroreductase. Zebrafish 2014;11:85–97. https://doi.org/10.1089/zeb.2013.0937.

Norges miljø- og biovitenskapelige universitet
Noregs miljø- og biovitskapelege universitet
Norwegian University of Life Sciences

Postboks 5003
NO-1432 Ås
Norway